creative commons
COMMONS DEED

저작자표시-비영리-변경금지 2.0 대한민국

이용자는 아래의 조건을 따르는 경우에 한하여 자유롭게

- 이 저작물을 복제, 배포, 전송, 전시, 공연 및 방송할 수 있습니다.

다음과 같은 조건을 따라야 합니다:

저작자표시. 귀하는 원저작자를 표시하여야 합니다.

비영리. 귀하는 이 저작물을 영리 목적으로 이용할 수 없습니다.

변경금지. 귀하는 이 저작물을 개작, 변형 또는 가공할 수 없습니다.

- 귀하는, 이 저작물의 재이용이나 배포의 경우, 이 저작물에 적용된 이용허락조건을 명확하게 나타내어야 합니다.
- 저작권자로부터 별도의 허가를 받으면 이러한 조건들은 적용되지 않습니다.

저작권법에 따른 이용자의 권리는 위의 내용에 의하여 영향을 받지 않습니다.

이것은 이용허락규약(Legal Code)을 이해하기 쉽게 요약한 것입니다.

Disclaimer

dCollection

연세대학교
YONSEI UNIVERSITY

Changes in Tribo-Mechanical Properties and Bacterial Resistance of Poly (Methyl Methacrylate) for 3D-Printed Intra-Oral Appliances by Incorporating Nanodiamonds

Utkarsh Mangal

The Graduate School
Yonsei University
Department of Dentistry

연세대학교
YONSEI UNIVERSITY

Changes in Tribo-Mechanical Properties and Bacterial Resistance of Poly (Methyl Methacrylate) for 3D-Printed Intra-Oral Appliances by Incorporating Nanodiamonds

A Dissertation
Submitted to the Department of Dentistry
and the Graduate School of Yonsei University
in partial fulfillment of the
requirements for the degree of
Doctor of Philosophy in Dental Science

Utkarsh Mangal

December 2021

연세대학교
YONSEI UNIVERSITY

This certifies that the Doctoral Dissertation
of Utkarsh Mangal is approved

Thesis Supervisor: Sung-Hwan Choi

Thesis Committee Member: Hyung-Seog Yu

Thesis Committee Member: Kee-Joon Lee

Thesis Committee Member: Jung-Yul Cha

Thesis Committee Member: Jae-Sung Kwon

The Graduate School

Yonsei University

December 2021

연세대학교
YONSEI UNIVERSITY

Acknowledgment

"*A journey of thousand miles begins with a single step.*" The successful completion of my Ph.D. program has been the first step in my academic career journey. For this vital first step, I shall always be immensely grateful.

Foremost, I would like to express my sincere gratitude to my advisor *Prof. Sung-Hwan Choi* for the continuous support of my Ph.D. study and research, motivation, and patience, and for sharing his immense knowledge in research during the program. His guidance helped me progress in timely completion of the Ph.D. project and helped me grow into a confident research academician. I could not have imagined a better advisor and mentor for my Ph.D. study.

Besides my advisor, my sincerest gratitude to the thesis evaluation committee: *Prof. Hyung-Seog Yu, Prof. Kee-Joon Lee,* and *Prof. Jung-Yul Cha* for their insightful comments and constructive criticism, which helped improve this thesis.

My sincere thanks also extend to *Prof. Jae-Sung Kwon*, who has been instrumental in helping me understand the nuances of dental biomaterial science and the use of 3D printing. The opportunity to translate theoretical knowledge from lectures into research has been of great help throughout the research program.

I thank my fellow lab mates, *Dr. Myung-Jin Lee, Ji-Young Seo, Ji-Yeong Kim, Jie Jin, Ji-Hoi-Kim* and *Jae-Hun Yu,* for stimulating discussions and teamwork. I should not miss mentioning the friends and guardians, at home and especially in Korea, who were willing to lend their ears and their words of encouragement.

Last but not least, I would like to thank my family: my parents, *Ms. Dipti Mangal, Dr. Narendra Mangal*, and my sister, *Ms. Niraly Mangal*, for their sacrifices, unconditional love and supporting me throughout my life.

Utkarsh Mangal
December 2021

연세대학교
YONSEI UNIVERSITY

TABLE OF CONTENTS

연세대학교
YONSEI UNIVERSITY

연세대학교
YONSEI UNIVERSITY

LIST OF FIGURES

연세대학교
YONSEI UNIVERSITY

LIST OF TABLES

연세대학교
YONSEI UNIVERSITY

ABSTRACT

Changes in Tribo-Mechanical Properties and Bacterial Resistance of Poly (Methyl Methacrylate) for 3D-Printed Intra-Oral Appliances by Incorporating Nanodiamonds

Utkarsh Mangal

Department of Dentistry, The Graduate School Yonsei University

(Directed by Professor Sung-Hwan Choi, D.D.S, Ph.D.)

3D printed intraoral devices must withstand mechanical and biological damage in the harsh environmental conditions of the oral cavity. In this study, aminated nanodiamonds (A-ND) with excellent properties such as high strength, chemical stability, and excellent biocompatibility were mixed with an acrylate-based 3D printing material, and their physical, mechanical, and biological properties were evaluated.

연세대학교
YONSEI UNIVERSITY

A UV-curable acrylate-based resin was used for the experiments. It was mixed with high-purity nanodiamonds (ND), and A-ND dispersed using chloroform in 0.1 wt. % to prepare a nanocomposite containing high-purity ND and A-ND. The unmodified resin was regarded as a control for comparison with ND and A-ND incorporated resins.

Compared to ND nanoparticles, A-ND nanoparticles were uniformly dispersed when mixed with resin, reducing agglomeration. ND and A-ND nanocomposites showed statistically significantly lower contact angle ($p < 0.001$) and solubility ($p < 0.05$) compared to the control group. The nanocomposite containing A-ND had significantly increased flexural strength ($p < 0.001$), elastic modulus ($p < 0.01$), and impact strength ($p < 0.001$) compared to the nanocomposite containing ND and the control group. In the nanocomposite group, the Vickers hardness of the surface increased statistically significantly ($p < 0.001$). In addition, significant improvement ($p < 0.001$) was confirmed in flexural strength, elastic modulus, and surface hardness after accelerated aging by thermocycling.

Friction and abrasion resistance tests were performed using stainless steel and titanium spheres as abrasive counterparts. The results showed that the friction coefficient of the ND and A-ND nanocomposite groups was significantly lower ($p < 0.01$) than that of the control group. However, when the titanium was used as the counterpart, the friction coefficient of the control group was similar to that of A-ND, but lower for ND. Both the ND and A-ND nanocomposite groups using stainless steel and titanium counterparts had improved abrasion resistance compared to the control group ($p <0.001$). In addition, A-ND

연세대학교
YONSEI UNIVERSITY

and ND displayed significantly enhanced resistance to *Streptococcus mutans* biofilm formation after 48 hours, compared to the control group ($p < 0.01$). Accuracy analysis of 3D printing orthodontic bracket analogs made of A-ND- and ND-nano composites was performed, and it was confirmed that there was no significant difference.

Therefore, it could be concluded that 0.1 wt. % of A-ND mixed with UV-polymerized polymethyl methacrylate (PMMA) resin markedly improved the mechanical and bacterial resistance while being faithful to the print accuracy and thus can be suitably used as a biomedical 3D printing material.

Keywords: poly (methyl methacrylate); nanodiamond; nanocomposites; 3D printing; mechanical properties; friction; wear resistance; *Streptococcus mutans*

연세대학교
YONSEI UNIVERSITY

Changes in Tribo-Mechanical Properties and Bacterial Resistance of Poly (Methyl Methacrylate) for 3D-Printed Intra-Oral Appliances by Incorporating Nanodiamonds

Utkarsh Mangal

Department of Dentistry, The Graduate School Yonsei University

(Directed by Professor Sung-Hwan Choi, D.D.S, Ph.D.)

I. INTRODUCTION

1. Digital dentistry and 3D printing

Digital dentistry has been increasingly applied due to the development of practical solutions in 3D scanning and printing. The application of digital technologies has prompted a reduction in the lead time for the manufacture of products such as splints, dental and maxillofacial prosthesis (Fernandes et al., 2016), scaffolds for guided tissue

연세대학교
YONSEI UNIVERSITY

regeneration (Carter et al., 2017), and intra-oral orthodontic appliances (Al Mortadi et al., 2015). Recent studies have also emphasized that the accuracy of the 3D-printed products is at par with the conventional methods, thus highlighting advantages such as reduced material demand and waste (Atzeni and Salmi, 2012), which decrease the carbon footprint (van Noort, 2012).

2. Poly(methyl methacrylate) in 3D printing

Although the technical aspects like 3D design of the appliance, and the 3D printer specifications play a vital role, the properties of the biomaterial used for printing are a significant factor in the adaptability and final application. Polymers like poly(methyl methacrylate) (PMMA) have been readily applied to additive manufacturing due to favorable properties such as formability, biocompatibility, and cost-effectiveness (El Bahra et al., 2013). However, the pure polymer products fabricated by 3D printing lack strength and hardness, thus limiting their long-term application in load-bearing or functional parts (Wang et al., 2017). These limitations are also experienced with PMMA-based 3D-printed dental appliances, such as orthodontic attachments, brackets, and provisional crowns, which require frequent replacement due to surface damage or loss of structure (Park et al., 2018).

In addition to the physical aspects of the surface integrity of intra-oral appliances, changes in the surface topography of polymers occur during the operation of these devices. In a microbial-rich oral environment, changes in the scale of roughness impact

연세대학교
YONSEI UNIVERSITY

the local microenvironment. Moreover, the physicochemical factors have the compound effect of enabling biofilm formation and bacterial attachment (Cheng et al., 2019). Furthermore, near-surface hydrodynamic interactions directly impact the efficacy of bacterial colonization. The existence of the hydrophilic surface results in the development of an air-liquid interface that interferes with the anchorage of bacterial appendages (Epstein et al., 2012).

3. Nanodiamond as filler additive

In recent years, several studies have emphasized a method for overcoming these limitations by reinforcing the polymer matrix with various types of fillers, thus leading to the development of high-strength nanocomposites (Aghajani Derazkola and Simchi, 2018; Yu et al., 2017). Noteworthy progress toward improving polymer properties has been made through the application of carbon-based nanofillers (CBNs), such as carbon nanotubes, graphene, and nanodiamonds (NDs) (Feng et al., 2019; Karami et al., 2019). In particular, NDs mimicking the properties of the bulk diamond, exhibit superior strength, high modulus, and excellent biocompatibility (Mochalin et al., 2012). These characteristics have enabled the use of NDs to considerably improve the bulk properties of the polymers, including PMMA, even in low ND concentrations (< 0.5 wt.%) (Al-Harbi et al., 2019; Protopapa et al., 2011). Moreover, the rich surface chemistry of the NDs imparts an inherent hydrophilicity of the ND at higher surface reactivities (Karami et al., 2019). The improved mechanical properties and increased surface hydrophilicity of the ND-reinforced composites have been observed (Waheed et al., 2019).

연세대학교
YONSEI UNIVERSITY

4. Functionalization and homogenization of nanodiamond

A good ND homogeneity in the polymer matrix is essential for ensuring consistent improvements through the incorporation of NDs. In addition to good dispersion, factors such as the nature of the nanofiller/polymer interface are critical for improving the properties (Balazs et al., 2006). Pristine NDs present a variety of oxygen-rich functional moieties that enable the surface chemistry of the ND to be tailored in order to expand its properties. Among the various moieties functionalized onto an ND surface, two functional groups that are stable in biomedical-research application are the carboxylic acid (-COOH) and amino ($-NH_2$) groups. In recent years, various research groups have attempted to incorporate aminated nanodiamonds (A-NDs) into polymers in order to enhance their mechanical properties, with varying degree of success reported (Karami et al., 2019; Mochalin et al., 2012). Polymers of lactic acid (Zhang et al., 2011) and epoxides (Neitzel et al., 2012a) have experienced definite improvements with A-NDs as nanofillers, although acrylate-based polymers have hardly been explored, especially acrylate-based 3D printed materials.

5. Research objective and null hypothesis

Even though the bulk properties ensure the integrity of the appliance, the polymer-based dental appliance experiences repeated insults in the form of abrasion and surface wear. This surface insult either occurs as two-body, three-body, or adhesion wear,

연세대학교
YONSEI UNIVERSITY

which is observed during chewing, tooth brushing, or between two components of an orthodontic appliance (e.g., brackets and wires), respectively (Ilie et al., 2017).

Taking this into account, the present study was conducted to evaluate the efficacy of A-NDs as nanofiller in biological-grade acrylate-based 3D printed materials with the aim of creating 3D-printed intraoral appliances that can withstand the physical stresses of the complex oral environment. We evaluated the tribo-mechanical properties of the ND-incorporated PMMA-based 3D-printed materials to characterize the changes in bulk mechanical properties and response to surface wear. We also investigated the resultant bacterial resistance of 3D-printed PMMA containing NDs. The following null hypothesis was considered: there will be no differences in properties between PMMA, PMMA-incorporated with NDs, and PMMA-incorporated with A-NDs, including the quality of additive-manufactured samples.

연세대학교
YONSEI UNIVERSITY

II. MATERIALS AND METHODS

1. Materials

The acrylate-based resin PMMA material (Class IIa material, viscosity: 0.8–1.15 Pa, relative density: *ca.* 1.15, NextDent Ortho Rigid, 3D Systems, NextDent B.V., Soesterberg, The Netherlands) was used in all the experiments. The PMMA resin is more soluble in organic solvents. The resin is chemically composed of methacrylic oligomers (>90% w/w) containing UV-sensitive (Blue UV-A 315–400) initiators for polymerization.

ND powder and anhydrous aminated ND (A-ND) powder were purchased from Tokyo Chemical Industry (TCI Co., Ltd. Tokyo, Japan), with purities greater than 97%. The as-received ND powder was gray in color, with an average particle size < 10 nm.

2. Specimen preparation

The ND-incorporated and A-ND-incorporated nanocomposites were prepared using purified ND and A-ND, respectively, at 0.1 wt.% of the neat resin. The pre-weighted ND powders were mixed with resin oligomers to achieve a homogenous distribution of the ND and A-ND. A solution-based mixing technique was also used with the help of high-power probe sonication in combination with magnetic stirring to achieve the same. The resin was degassed in vacuum for 2 h and used without any further modification to print the substrate specimens.

연세대학교
YONSEI UNIVERSITY

The nanoparticles were dispersed in the polymer matrix by solution-based mixing using chloroform ($CHCl_3$, Sigma-Aldrich, St. Louis, MO, USA) (Prolongo et al., 2008). The purified or A-ND suspension in chloroform was stirred at 50 °C for 30 min and then probe-sonicated using with a 50–60 Hz sonicator (Q125, Qsonica, LLC., Newtown, CT, USA). The neat resin was magnetically stirred at 60 °C for 30 min to lower its viscosity. To promote homogenous dispersion, the suspension was then mixed with a predetermined weight of the low viscosity resin and magnetically stirred for 24 h at 60 °C, after which the solvent was slowly evaporated over 2 d with continuous stirring (500 rpm) at 60 °C. The resultant ND-resin suspension was degassed under vacuum and used as is.

All specimens were fabricated using a digital light processing (DLP) 3D printer (NextDent 5100, 3D Systems, NextDent B.V., Soesterberg, Netherlands) with the stereolithography data for each specimen prepared according to the measurement method using 3D design and modelling software (Autodesk® Meshmixer, Autodesk, San Rafael, CA, USA). The specimens were polymerized under 405 nm light at a maximum printing speed setting of 140 mm/h and post-cured (15 min) according to the manufacturer's instructions using a UV oven (NextDent LC-3DPrint Box, 3D Systems, NextDent B.V., Soesterberg, The Netherlands) (Figure 1).

Three groups were compared for all the experiments viz. (i) control; PMMA resin as supplied by the manufacture with no modifications, (ii) ND; PMMA resin augmented with 0.1 wt.% of nonfunctionalized ND, and (iii) A-ND; PMMA resin augmented with 0.1 wt.% of amine functionalized nanodiamond.

연세대학교
YONSEI UNIVERSITY

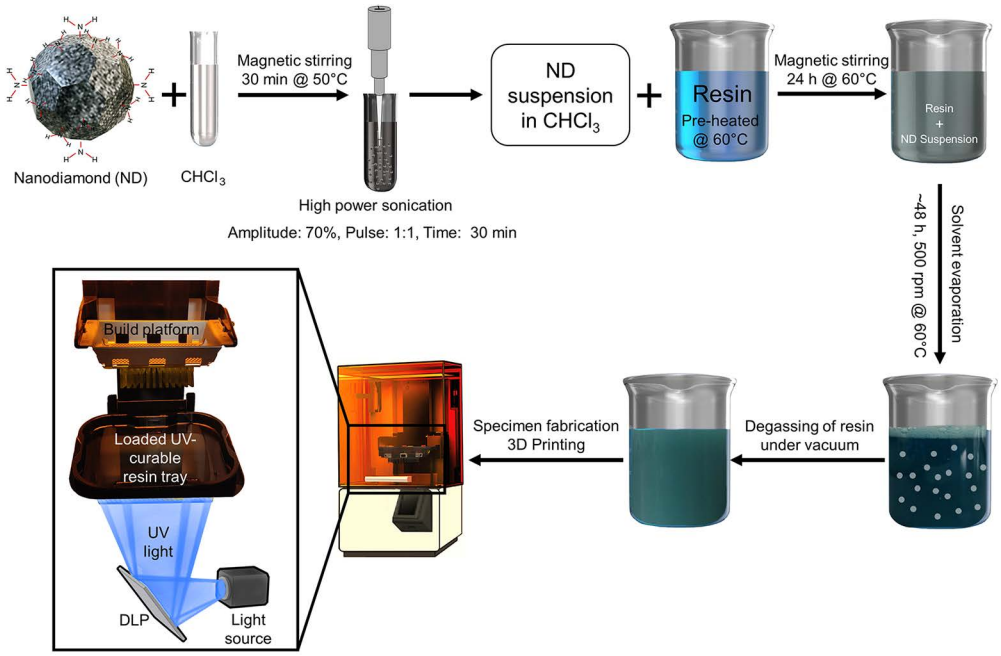

Figure 1. Schematic representation of the fabrication protocol. Solution based mixing of nanodiamond particles in low weight percentages enables relatively homogenous dispersion. Vacuum degassing ensures stable quality of additively manufactured specimens.

연세대학교
YONSEI UNIVERSITY

3. Characterizing the ND- and A-ND incorporated nanocomposites

Transmission electron microscopy (TEM; JEM-200F, JEOL, Tokyo, Japan) was used to qualitatively characterize the aggregation tendency of the NDs and A-NDs in resin. To that end, 0.1 mg of each sample was dispersed in 1 mL of ethanol and one drop of the suspension was deposited on a TEM grid (200 mesh) and dried under vacuum. Images were acquired at 200 kV. To quantitatively compare the aggregation tendency of the NDs and A-NDs, 1 mg/mL of each sample was measured by dynamic light scattering with Zetasizer Nano ZS90 (Malvern Instruments Ltd, Malvern, United Kingdom).

The control and the ND- and A-ND-incorporated samples, along with the ND nanofillers themselves were subjected to Fourier-transform infrared (FT-IR) spectroscopy (Nicolet™ iS™ 10 FTIR spectrometer, Thermo Fisher Scientific, Korea). Each sample was washed twice with ethanol to remove impurities prior to the acquisition of its spectrum.

For thermogravimetric analysis (TGA), a TG/DTA7300 (Seiko Instruments Inc. Chiba, Japan) was employed. TGA was performed on the ND and A-ND nanodiamond powder, the control and ND- and A-ND-incorporated samples, in the presence of nitrogen. The equilibration at 100 °C for 20 minutes was followed by a ramp of 10 °C/min up to 800 °C. A total of 2-5 mg of each sample was weighed and placed in an alumina crucible for analysis.

연세대학교
YONSEI UNIVERSITY

The nano-polymerized specimens were characterized by examining their surface morphologies and fracture-surface patterns created with a computer-controlled universal testing machine at a crosshead speed of 5 mm/min. Field-emission scanning electron microscopy (FE-SEM) images were acquired on a JEOL-7800F microscope (Tokyo, Japan). All samples were coated with 5-nm-thick Pt using an ion coater (ACE600, Leica, Wetzlar, Germany).

4. Water contact angle

The contact angles of the samples (n = 5) were measured to evaluate the hydrophobicities/hydrophilicities of the ND- and A-ND-incorporated nanocomposites. The contact angle θ was determined by measuring the angle between the examined flat surface and the tangent created by a drop of dH_2O at the point of contact with the surface. To that end, dH_2O (3 μL) was placed at 1.0 $\mu L \cdot s^{-1}$ at the center of each sample surface at room temperature. Contact angles were measured using a droplet analysis device (SmartDrop, Femtofab, Seongnam-si, Korea) and the sessile-drop method.

5. Water sorption and solubility

Disc-shaped specimens (d = 15.0 mm, h = 1.0 mm, n = 5) were prepared for each group in accordance with a previously reported method (Lee et al., 2019). The specimens were kept in a desiccator maintained at 37 ± 2 °C for 22 h, after which they were transferred into another desiccator maintained at 23 ± 1°C for 2 h and weighed to an accuracy of ± 0.1 mg. The initial mass (m_1) was recorded when the mass of the specimen

연세대학교
YONSEI UNIVERSITY

did not change by more than 0.1 mg in any 24 h period. After final drying, the mean diameter and thickness of each specimen was measured to an accuracy of ± 0.01 mm and the volume of the sample was calculated (V; mm^3). Each specimen was immersed in 15 mL of distilled water at 37 ± 1 °C for 7 d. The surface water was removed by blotting to eliminate any visible moisture, after which each specimen was waved about in the air for 15 s and weighed (m_2) within 60 s of its removal from the water. The specimens were then stored in desiccators as described above until a constant mass (m_3) was achieved. The water sorption ((m_2–m_3)/V) and the water solubility ((m_1–m_3)/V) values were then calculated.

6. Strength and modulus

In the present study, mechanical properties were analyzed following the ISO 20795-2 International Standard, which is related to the specific applications of the PMMA of interest in this study, namely orthodontic appliances. Eighteen samples (n = 6, control, ND-, and A-ND-incorporated) were printed and sequentially polished (800,1000,1200 grit) to average dimensions of 3.3 mm × 10 mm × 64 mm. A computer-controlled universal testing machine (Model 3366, Instron, Norwood, MA, USA) was used to fracture the specimens through three-point flexure with a 1 kN load cell. The flexural strength (σ_f), elastic modulus (E_f) and modulus of resilience (Ur) were measured at a span length of 50 mm and a crosshead speed of 5 mm/min. The following equations were used to perform the calculations:

연세대학교
YONSEI UNIVERSITY

$$\sigma_f = \frac{3Fl}{2bh^2} \quad (1)$$

$$E_f = \frac{F_1 l^3}{4bh^3 d} \quad (2)$$

$$Ur = \sigma_f^2 / 2.E_f. \quad (3)$$

where,

F is the maximum load, in newtons, exerted on the specimen;

l is the distance, in millimetres, between the supports, accurate to ± 0,01 mm;

b is the width, in millimetres, of the specimen measured immediately prior to water storage;

h is the height, in millimetres, of the specimen measured immediately prior to water storage;

*F*1 is the load, in newtons, at a point in the straight-line portion (with the maximum slope) of the load/deflection curve;

d is the deflection, in millimetres, at load *F*1.

Impact strength was determined by the IZOD impact test according to a modified ASTM D256 specification. Ten unnotched rectangular specimens (l = 64 mm, h = 12.7, and b = 3.2 mm) were printed. The specimens were then subjected to impact testing using an IZOD impact apparatus (Yasuda Seiki Seisakusho Ltd., Tokyo, Japan) with a swinging

연세대학교
YONSEI UNIVERSITY

pendulum (0.598 g, 0.33 m). Impact strength is expressed as energy per unit and calculated using the formula: $IS = E/hb$, where E is the absorbed energy calculated as the difference between the nominal and dynamic energy of the pendulum after specimen fracture.

7. Microhardness

The surface microhardness was determined using a Vickers hardness tester (DMH-2, Matsuzawa Siki Co. Ltd., Akita, Japan) with a force of 300 gf (2.94 N) for 30 s. Six indentations, spaced at least 1 mm from each other, were made on each specimen, resulting in 30 indentations per group (n=5).

8. Tribological analysis

A ball-on-flat configuration was used to conduct the tribological tests using a reciprocating tribometer and the conditions were adapted from earlier studies (Neitzel et al., 2012a; Yu et al., 2017). The holder was designed to house the antagonists through which the normal load was applied to the 3D-printed specimens (cuboidal: x × y × z: 20× 20×3.5 mm).

8.1 Coefficient of friction and wear resistance

In this study, the balls with 5 mm diameter, made from either stainless steel (SS; SUS 304) or grade V titanium alloy (TI; Ti-6Al-4V) were used as the antagonists. The experiment design included a vertical load of 5 N, with a reciprocating amplitude of 2

연세대학교
YONSEI UNIVERSITY

mm and a frequency of 0.5 Hz. A total of 10^4 cycles were performed, recording a total sliding distance of 40 m, under PBS lubrication. The conditions were designed to reflect the low frequency and amplitude in the range of values of intraoral chewing parameters as identified in the literature (Zhou et al., 2013). The reported average coefficient of friction (COF) was calculated from the data collected.

8.2 Wear morphology characterization

The wear scars after the reciprocating test were analyzed using 3D confocal laser scanning microscopy (CLSM, VK-X200, Keyence, Japan). The wear rate and corresponding wear area were determined from each scan. The corresponding wear scars were further qualitatively evaluated using imaging 3D optical profilometry (ContourGT-X 3D Optical Profiler, Bruker, Billerica, MA, USA) in non-contact mode at 50× objective.

9. Hydro-thermal fatigue testing

To simulate accelerated physiological aging of the nanopolymers, the commonly employed method of thermocycling was used (Gale and Darvell, 1999). Specimens with same design as in mechanical testing were prepared and stored dry at 23 ± 2 °C for 24 ± 2 h. Since there is no definite standardization for bath temperatures or for number of cycles for thermocycling, the recurrently used method advocated by the International Organization for Standardization (ISO)/TS 10477:2018 for testing dental materials was used. All thermocycles were conducted between 5 °C and 55 °C for a dwell time of 30 s.

연세대학교
YONSEI UNIVERSITY

Time of filling and emptying the vessel with a working liquid (water) was 15 s for a total of 5000 cycles (RB 508, Thermal Cyclic Tester, R&B Inc, Daejeon, Korea).

10. Bacterial resistance

The strain used in the experiment was *Streptococcus mutans* (*S. mutans*, ATCC 25175), and the previously established protocol for the biofilm culture was followed (Kwon et al., 2019; Thaweboon and Thaweboon, 2019). The frozen bacterial colonies of *S. mutans* were thawed and cultured in sucrose supplemented (5%) Brain Heart Infusion broth (BHI, Becton Dickinson and Co., Sparks, MD, USA) at 37 °C for 24 h. The bacterial suspension (200 μL) was then added to the wells containing 3D-printed disk-shaped specimens and maintained at 37 °C for 120 min in a shaking incubator. Following three consecutive washes with the phosphate buffer saline solution (PBS), the sucrose supplemented BHI (200 μL) was added and further incubated at 37 °C.

The biofilms could grow for a total of 48 h. The specimens were stained using the live/dead cell viability kit (Molecular Probes, Eugene, OR, USA). Equal volumes of the SYTO 9 dye and propidium iodide obtained from the kit, which stain live (green) and dead (red) organisms, respectively, were mixed thoroughly. A 3 μL aliquot of this mixture in PBS was used to stain the samples. The stained samples were incubated at room temperature in the dark for 15 min. Images of the axially stacked biofilm were captured using CLSM (LSM700, Carl Zeiss, Thornwood, NY, USA), and the thickness of the biofilm was calculated using the software ZEN (Carl Zeiss, Thornwood, NY, USA).

연세대학교
YONSEI UNIVERSITY

Additionally, the COMSTAT plug-in for the Image J (NIH, Bethesda, MA, USA) software was used to determine the average biomass (Heydorn et al., 2000).

11. Additive manufacturing trueness

Fifteen orthodontic bracket-shaped specimens (n = 5, control, ND-, and A-ND-incorporated) were 3D printed (NextDent 5100, 3D Systems, NextDent B.V., Soesterberg, Netherlands). The samples were then scanned using a 3Shape E3 scanner (3Shape, Copenhagen, Denmark). To minimize the errors while scanning printed samples the simulated orthodontic bracket design was upscaled. Dimensional accuracies were evaluated for the three groups against a reference computer-aided-design file used for printing brackets. The best-fit superimposition method using a 3D morphometric program (Geomagic® Control X™, 3D Systems, Rock Hill, SC, USA) was used to determine root mean square deviation (RMS) values that indicate trueness between samples (Kim et al., 2018). Overall deviations were shown on a color map for intuitive comparison with deviations of ±200 μm and tolerances of ±10 μm assigned.

12. Statistical analysis

All statistical analyses were performed using IBM SPSS software, version 25.0 (IBM Korea Inc., Seoul, Korea) for Windows, with data from at least three independent experiments. The results obtained from the control and experimental groups were analyzed by one-way analysis of variance (ANOVA) followed by Tukey's test. $p < 0.05$ was statistically significant.

연세대학교
YONSEI UNIVERSITY

III. RESULTS

1. Characterizing ND- and A-ND incorporated nanocomposites

TEM images of the ND- and A-ND-containing resins show particles that are 4–6 nm in size and are aggregated in both materials; however, the NDs appear to be more aggregated than the A-NDs. The particles in the latter are somewhat more homogeneously dispersed, as is evident in Figure 2A.

To observe the aggregation tendency and cluster size distribution, particle size analysis was conducted. The results from dynamic light scattering showed marked differences between the NDs and A-NDs, as appreciated in the histograms in Figure 2B. The NDs showed an aggregation tendency with size more than 100 nm having 62.1% of aggregates in size range of 160-255 nm and 8.8% of aggregates greater than 1 μm in size. In contrast, with A-NDs 90% of the aggregates were found in the size range of 20-40 nm.

연세대학교
YONSEI UNIVERSITY

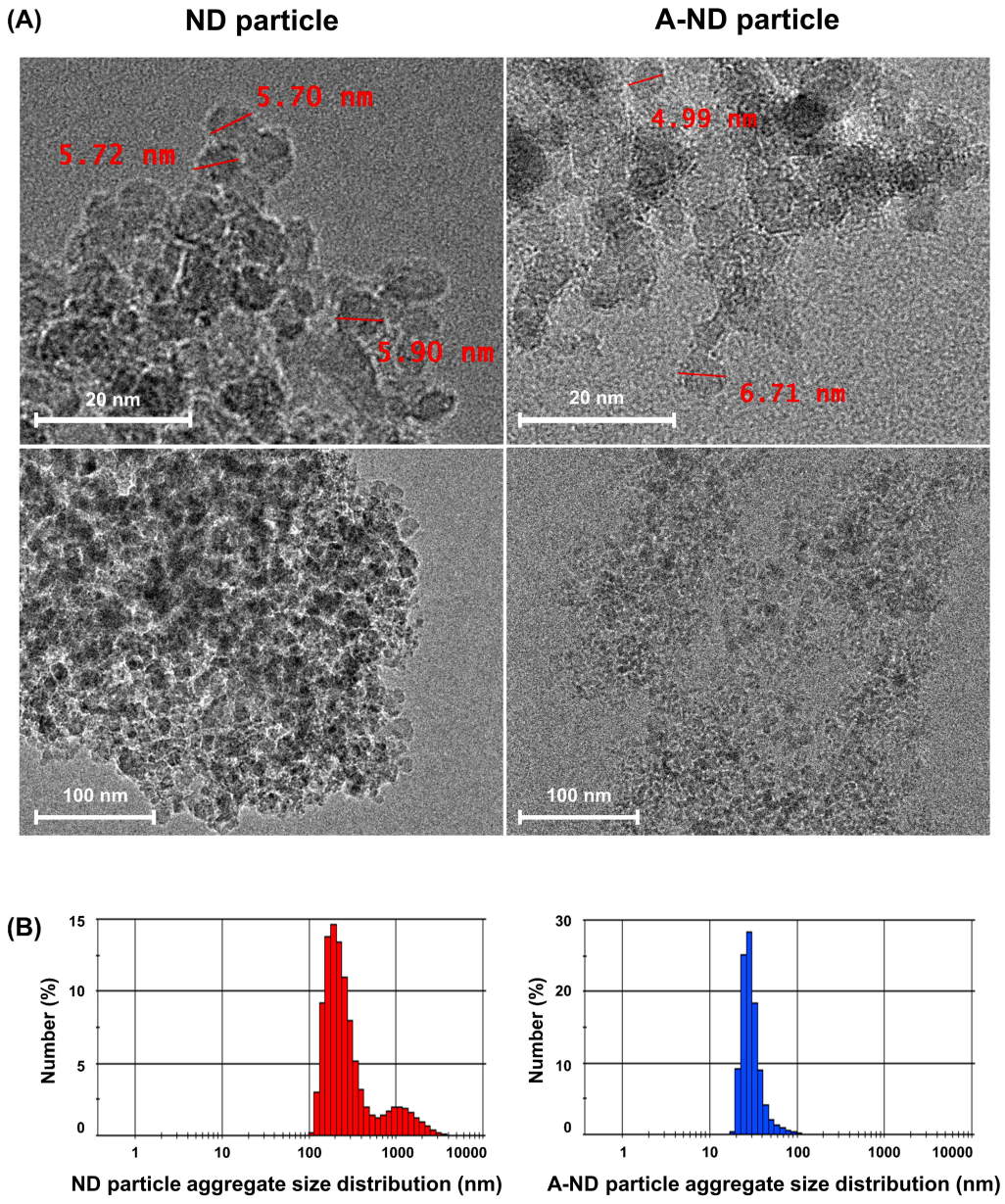

Figure 2. Morphological characterization of nanodiamond particles. (A) TEM images of NDs and A-NDs, and (B) histograms showing aggregate size evaluation.

연세대학교
YONSEI UNIVERSITY

The FT-IR spectra of the nanofiller powders and polymerized specimens are displayed in Figures 3A and 3B, which reveals the presence of bands at 2815–2964 cm^{-1} (C—H stretching), 3448 cm^{-1} and 1554 cm^{-1} (N—H stretching and bending), and 1632 cm^{-1} (C=C) in the spectrum of the A-ND powder. The comparison of the FTIR spectra of powder of ND with A-ND (Figure 3A) shows a distinctive peak at 1554 cm^{-1}, which is observed in the IR spectrum of A-ND and absent in the spectrum of ND. This has been identified as the amide II band, a mixture of C—N stretch and N—H vibrations, reported in range of 1550 ± 20 cm^{-1} (Amides et al., 2003). The peak observed in 1630 ± 10 cm^{-1} both ND and A-ND can be assigned to the bending mode of O—H or N—H bonds.

In the higher frequency range maximum intensity in the 2800-3500 cm^{-1} can be observed as the red shift in the A-ND ($-NH_2$), described as the result of the overlap of the N—H stretch by Mochalin et al (Mochalin et al., 2011). The FT-IR spectra of the nanocomposites reveal characteristic bands that correspond to acrylate groups, with the main band (1730 cm^{-1}) attributable to carbonyl groups.

연세대학교
YONSEI UNIVERSITY

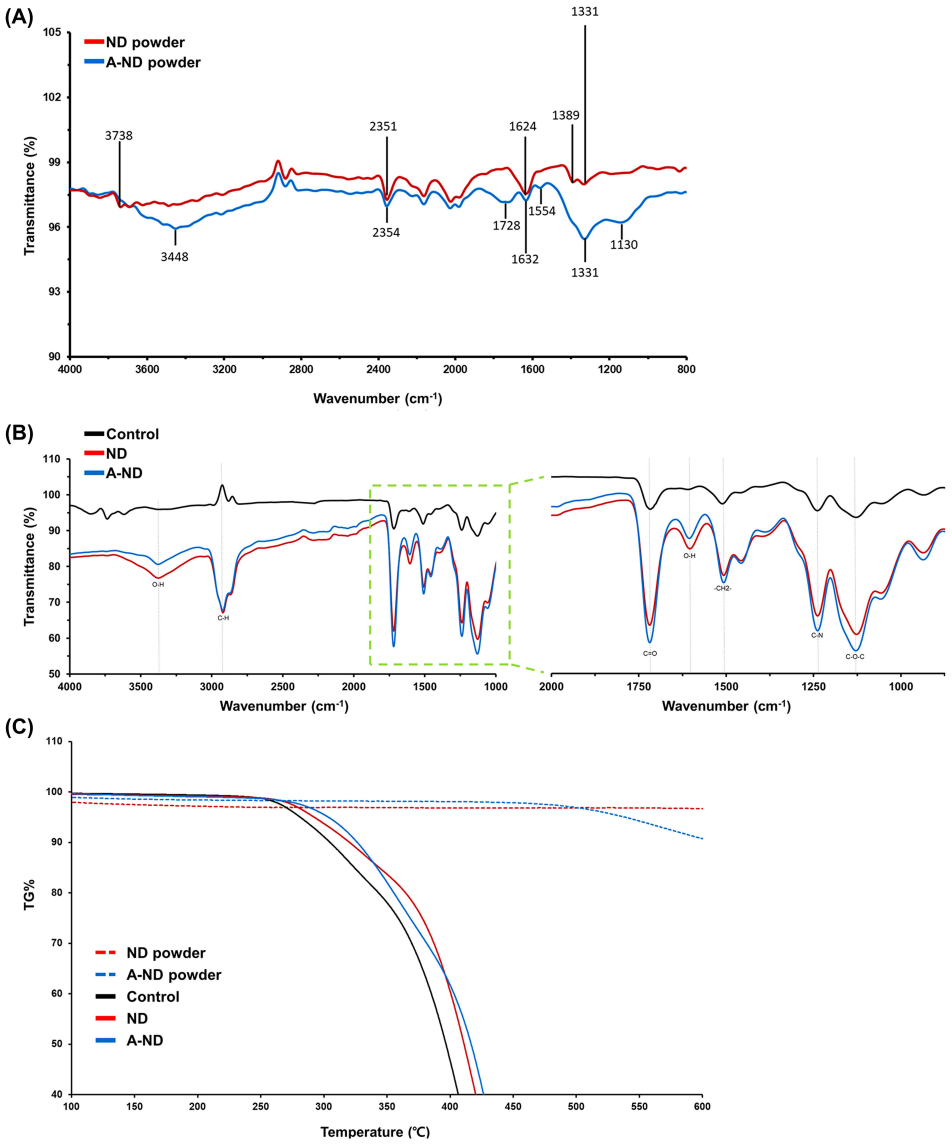

Figure 3. Spectroscopic and thermogravimetric characterization. (A) FT-IR spectra of the ND and A-ND powders, and (B) the control, ND- and A-ND-incorporated nanocomposites with expanded 1000–2000 cm $^{-1}$ regions shown. (C) TGA profile of the ND and A-ND powders, and the control and ND- and A-ND-incorporated samples.

연세대학교
YONSEI UNIVERSITY

As seen in Figure 3C, TGA curve for both ND and A-ND powder does not show any significant mass loss up to 500 °C, which approves the stable nature for such temperature interval. The TGA curve for the control exhibited a low thermal stability with a sharp drop in the weight loss from 270 °C compared to the ND- and A-ND incorporated nanocomposites, which showed higher thermal stability. In the control group, 40% of weight loss was recorded at 405°C while in the ND- and A-ND incorporated nanocomposites same was observed at 420 °C and 426 °C, respectively.

The smooth appearance of the macroscopically fractured section highlights the brittle nature of the control sample. The SEM images in Figures 4A and 4D reveal that the fracture surface of the control sample is smooth with minimal features. The fracture surfaces of the ND- (Figure 4B and 4E) and A-ND-incorporated samples (Figure 4C and 4F) show the impact of the nanofiller, as markedly rough surfaces were observed for both nanofiller-containing samples, confirming that high energy is required for crack propagation. Moreover, no microscale agglomeration was observed in the nanocomposite samples, on either their surfaces or fracture-surface cross-sections.

연세대학교
YONSEI UNIVERSITY

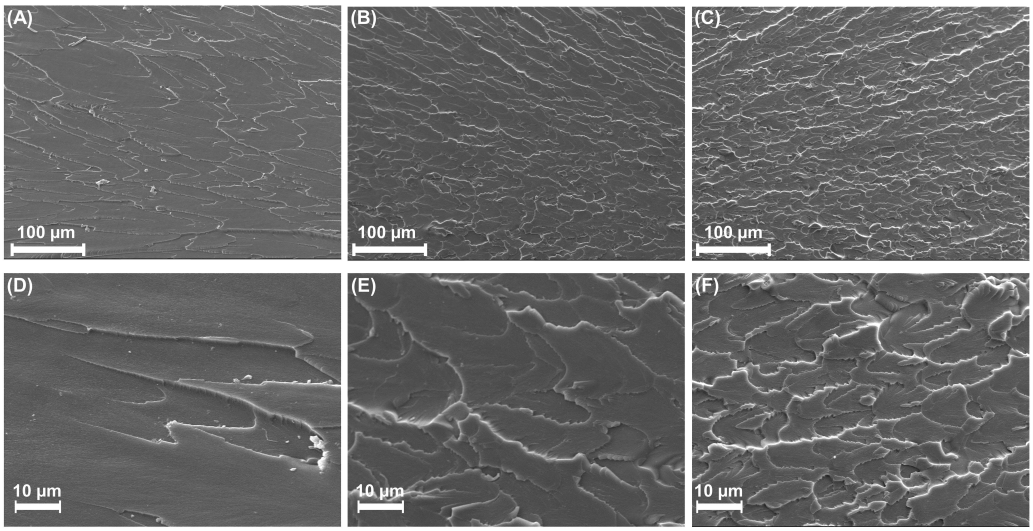

Figure 4. Characterization of fracture surface with SEM. Micrographs (A and D) the control, (B and E) ND-, and (C and F) A-ND-incorporated nanocomposites, showing distinct features in fracture-surface patterns. (A–C) 250 × and (D-F) 1000 × magnification.

연세대학교
YONSEI UNIVERSITY

2. Hydrophilicity, water sorption, and solubility

Wettability evaluated through contact-angle analysis revealed statistically significant differences between the control and nanocomposite groups ($p < 0.001$, Figure 5A). The average value of contact angle was highest for the control group (73.81° ± 4.9°), followed by the A-ND- (48.22° ± 8.01°) and ND-incorporated (17.32° ± 6.4°) groups.

The water sorption results (Figure 5B) show values that decrease from the control (22.55 ± 3.63 μg/mm^3) to the ND- (21.55 ± 2.44 μg/mm^3) and A-ND-incorporated (20.62 ± 0.78 μg/mm^3) groups; however, these values were not statistically significant. In contrast, the solubility results in Figure 5C show marked differences between the three groups (control: 0.168 ± 0.15 μg/mm^3; ND-incorporated: 0.024 ± 0.35 μg/mm^3; A-ND-incorporated: -0.348 ± 0.33 μg/mm^3); the difference between the control and A-ND-incorporated groups was found to be statistically significant ($p < 0.05$).

연세대학교
YONSEI UNIVERSITY

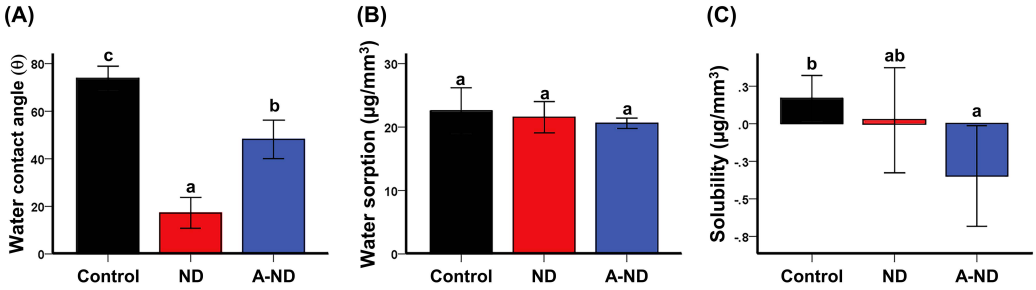

Figure 5. Surface physical properties as a factor of reaction with water. Comparing (A) water contact angles, (B) water sorption, and (C) water solubility of the control, ND-, and A-ND-incorporated groups. Statistical analysis with one-way ANOVA and post-hoc analysis with Tukey's test was conducted to compare the groups. Dissimilar letters indicate significant differences from each group ($p < 0.05$).

연세대학교
YONSEI UNIVERSITY

3. Mechanical properties of nanocomposites

The ND-incorporated test groups showed higher flexural and impact strengths compared to those of the control (Figures 6A and 6B; Table 1). Significant differences were observed for flexural strength and impact strength (A-ND > ND > control; $p < 0.001$) between all groups.

The A-ND-incorporated nanocomposite exhibited an elastic modulus that was significantly higher ($p < 0.01$) compared to those of both the ND-incorporated sample and the control, whose values were comparable and not markedly different (Figure 6C). However, both the ND- and A-ND-incorporated samples exhibited moduli of resilience that were significantly higher ($p < 0.001$) than that of the control, although the values for the ND- and A-ND-incorporated samples were not significantly different (Figure 6D).

연세대학교
YONSEI UNIVERSITY

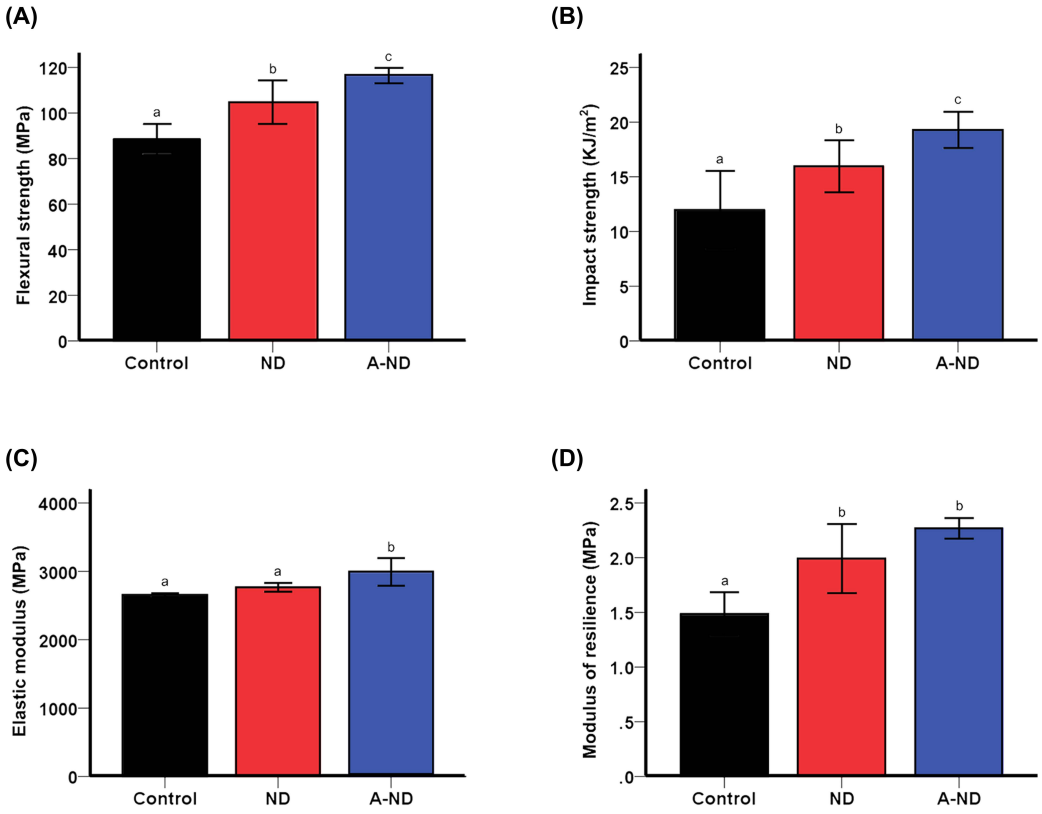

Figure 6. Mechanical properties of nanocomposites. Comparing the (A) flexural strengths, (B) impact strengths, (C) elastic moduli, and (D) moduli of resilience (D) of the various groups of samples. Statistical analysis with one-way ANOVA and post-hoc analysis with Tukey's test was conducted to compare the groups. Dissimilar letters indicate significant differences from each group ($p < 0.05$).

연세대학교
YONSEI UNIVERSITY

Table 1. Mean values of strength, and modulus of the various groups and their standard deviations (SDs).

Group	Flexural Strength (MPa)	Impact Strength (kJ/m^2)	Elastic Modulus (MPa)	Modulus of Resilience (MPa)
Control	88.53 ± 6.53^a	11.95 ± 3.56^a	2654.34 ± 25.23^a	1.48 ± 0.19^a
ND	104.78 ± 9.49^b	15.95 ± 2.38^b	2766.48 ± 61.03^a	1.99 ± 0.31^b
A-ND	116.38 ± 3.36^c	19.26 ± 1.66^c	2989.58 ± 200.28^b	2.26 ± 0.09^b

Statistical analysis with one-way ANOVA and post-hoc analysis with Tukey's test was conducted to compare the groups. In the vertical column, dissimilar letters indicate significant differences from each group ($p < 0.05$).

4. Tribological and surface mechanical properties

Tribological test were conducted for analysis two body type surface interaction (Figure 7A-B). The Vickers microhardness test used to examine the surface hardness of nanocomposites revealed that, with the addition of diamond nanoparticles, the hardness values of both ND (18.71 ± 1.25 kg/mm^2) and A-ND (17.80 ± 1.51 kg/mm^2) increased significantly compared to the control group (15.91 ± 1.27 kg/mm^2), with the difference being statistically significant ($p < 0.001$). However, at the present concentration of the nanofillers, there was no statistically significant difference ($p = 0.091$) when the NDs were applied (Figure 7C). The surface roughness analysis of cuboidal specimens preceding tribological testing had no significant differences between the mean surface roughness measured between the control (Ra: 0.47 ± 0.11 μm), ND (Ra: 0.48 ± 0.16 μm), and A-ND (Ra: 0.59 ± 0.13 μm) incorporated nanocomposites (Figure 7D).

연세대학교
YONSEI UNIVERSITY

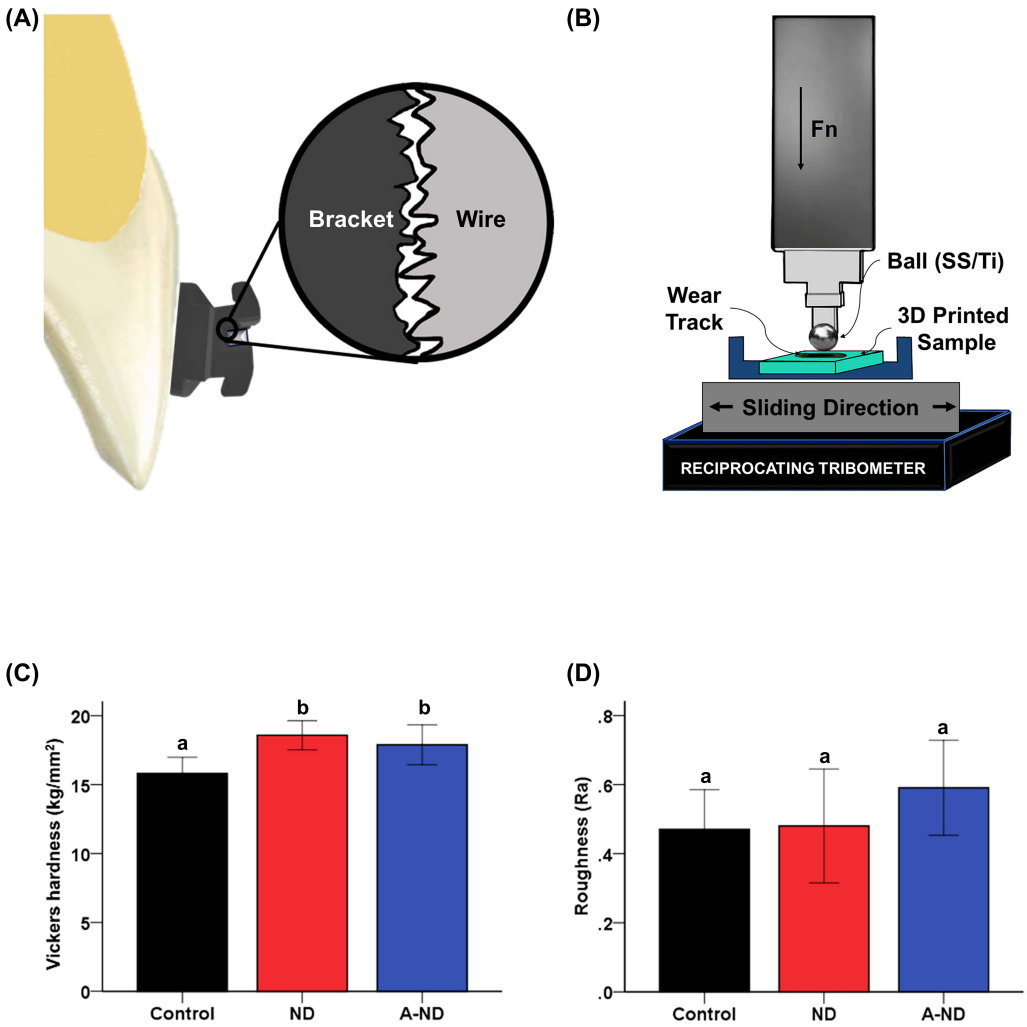

Figure 7. Analysis of microsurface mechanical interaction. (A) Surface interaction at the microlevel of an orthodontic bracket with the wire surface within the slot. (B) Schematic representation of the computer-controlled and adjustable reciprocating tribometer. Comparison of the (C) Vickers hardness and (D) surface roughness (μm) of the various groups of samples. Statistical analysis with one-way ANOVA and post-hoc analysis with Tukey's test was conducted to compare the groups. Dissimilar letters indicate significant differences from each group ($p < 0.05$).

연세대학교
YONSEI UNIVERSITY

4.1 Friction coefficient

Figure 8 shows the mean of the continuously recorded static friction coefficients calculated with the macroscopic test. Figure 8A and 8B depict the COF curves recorded in reciprocating mode for two nanocomposites and the control group against stainless steel and grade V titanium, respectively. Against the SS antagonist, after an initial period of 1000 cycles, a statistically significant ($p < 0.01$) increase in the COF could be observed in the control group specimens compared to the ND- and A-ND-incorporated nanocomposites specimens (Figure 8C).

In contrast, against the Ti antagonist, the control group demonstrated a gradual decrease in the COF to a value lower than those of both the ND- and A-ND-incorporated nanocomposites. Although the control and A-ND were statistically similar ($p = 0.065$), the average COF for the ND nanocomposite was significantly ($p < 0.01$) larger than that for the control after 10^4 cycles (Figure 8D).

연세대학교
YONSEI UNIVERSITY

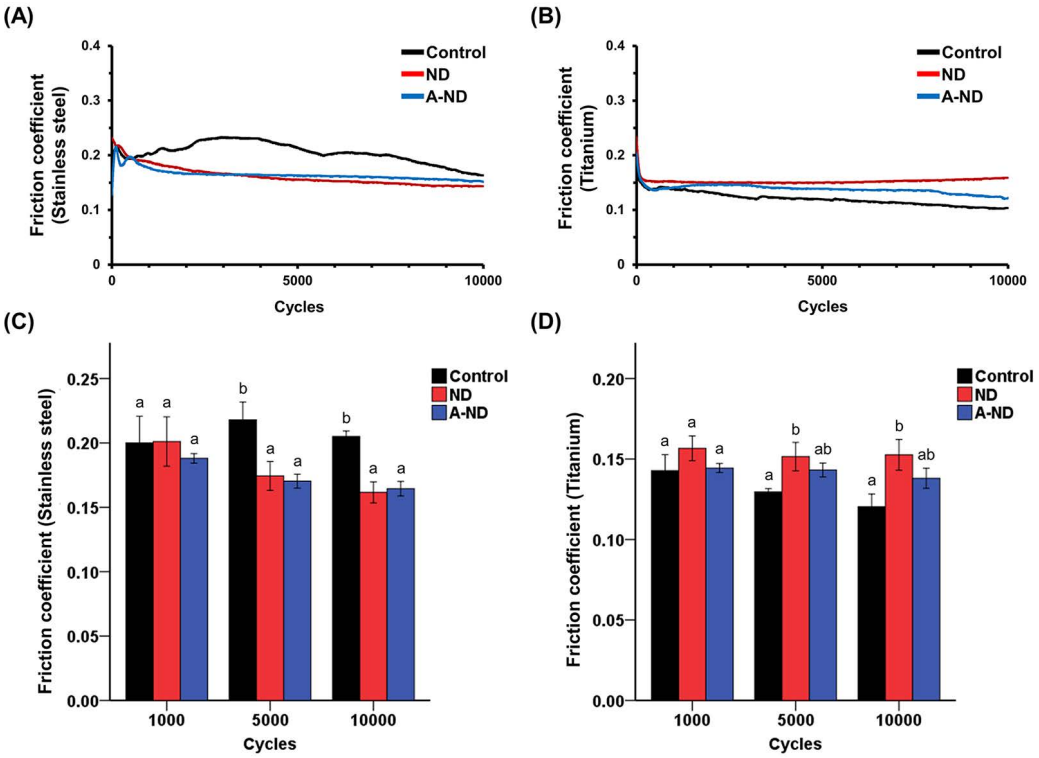

Figure 8. Dynamic coefficient of friction (COF) over reciprocal cyclic loading. Graphical representation of the contour diagram of the different groups against (A) stainless steel and (B) titanium. Comparison of the COF between the different groups after 1000, 5000, and 10000 cycles with (C) stainless steel and (D) titanium. Statistical analysis with one-way ANOVA and post-hoc analysis with Tukey's test was conducted to compare the groups. The friction coefficients were compared at three specific time points (completion cycles), such that dissimilar letters indicate significant differences from each group at the given cycle completion point ($p < 0.05$).

.

연세대학교
YONSEI UNIVERSITY

4.2 Wear rate

The wear rate comparison between the groups is shown in Figure 9. The analysis of the different groups demonstrated a significant difference ($p < 0.001$) in the wear rate with the addition of both ND and A-ND in the PMMA based polymer. Compared to that of the control group (SS: 2.14×10^{-8} mm^3/Nm; Ti: 1.15×10^{-8} mm^3/Nm), the specimens containing ND (SS: 1.04×10^{-8} mm^3/Nm; Ti: 0.49×10^{-8} mm^3/Nm) and A-ND (SS: 0.78×10^{-8} mm^3/Nm; Ti: 0.58×10^{-8} mm^3/Nm) exhibited a significant decrease in the wear rate, with both the SS and Ti counter surfaces. There was no significant difference in the wear rate between ND and A-ND for both the SS and Ti counter surfaces.

연세대학교
YONSEI UNIVERSITY

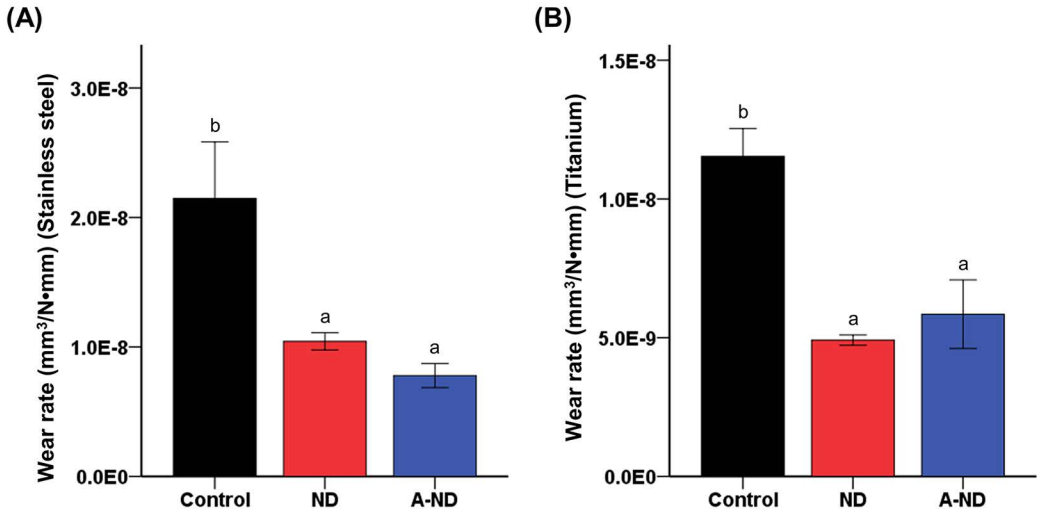

Figure 9. Wear behavior of the nanocomposites per unit area. Comparison of the wear rate of the control and nanocomposites against (A) stainless steel and (B) titanium. Statistical analysis with one-way ANOVA and post-hoc analysis with Tukey's test was conducted to compare the groups. Dissimilar letters indicate significant differences from each group ($p < 0.05$).

연세대학교
YONSEI UNIVERSITY

4.3 Wear area and morphology

The abrasive loss from the polymer substrate specimens represented by the wear area indicated a considerable improvement in the wear resistance against both SS ($p < 0.001$, Figure 10A) and Ti ($p < 0.01$, Figure 10B) with the addition of ND or A-ND. The control (SS: 2146.9 μm^2, Ti: 1154.1 μm^2) group revealed a significantly larger wear area compared to the PMMA specimens containing both ND (SS: 1042.38 μm^2, Ti: 736.71 μm^2) and A-ND (SS: 779.28 μm^2, Ti: 876.93 μm^2) (Figure 10C and 10D). There was no significant difference in the wear area between ND and A-ND for both the SS and Ti counter surfaces.

연세대학교
YONSEI UNIVERSITY

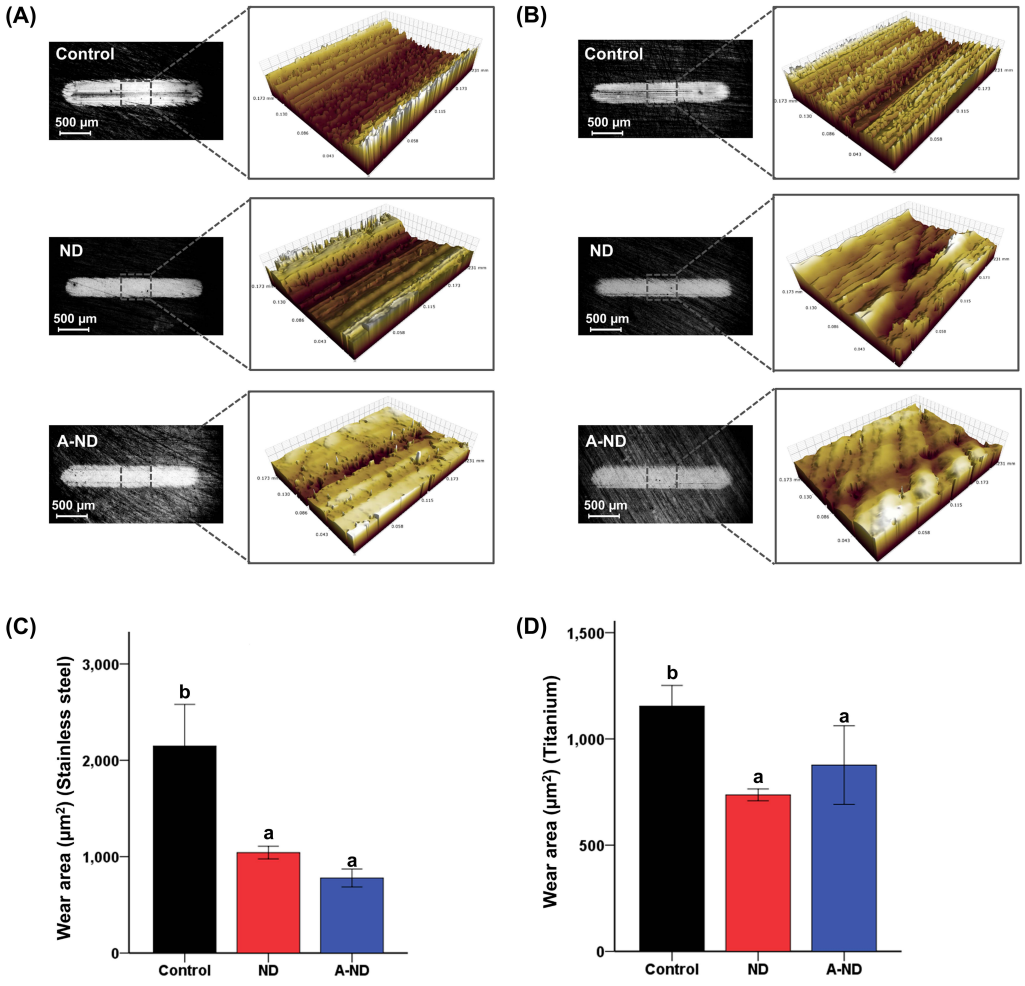

Figure 10. Wear area comparison of the control and nanocomposites. Representative image of the light microscopy and optical profilometer scans of the wear scar, in non-contact mode, for (A) stainless steel and (B) titanium. Statistical comparison of the wear area between the different test groups against, (C) stainless steel and (D) titanium. Statistical analysis with one-way ANOVA and post-hoc analysis with Tukey's test was conducted to compare the groups. Dissimilar letters indicate significant differences from each group ($p < 0.05$).

연세대학교
YONSEI UNIVERSITY

5. Response to hydro-thermal fatigue

Following 5000 thermocycles, comparison between the mechanical properties is summarized in Table 2, Figure 11. Flexural strength was significantly ($p < 0.001$) lower in control compared to both ND-incorporated and A-ND-incorporated nanocomposites; however, the nanocomposite groups were comparable. Elastic modulus was significantly ($p < 0.05$) lower in control when compared to A-ND--incorporated, whereas the ND-incorporated group had no significant difference in relation to both control and A-ND-incorporated nanocomposite. The modulus of resilience also showed similar trend as before thermocycling, however, the statistically significant increase was observed from control to ND to A-ND ($p < 0.001$).

Nanocomposites maintained significantly higher surface hardness than control group after thermocycling also. However, statistically significant differences were also observed in the A-ND group compared to the ND group.

연세대학교
YONSEI UNIVERSITY

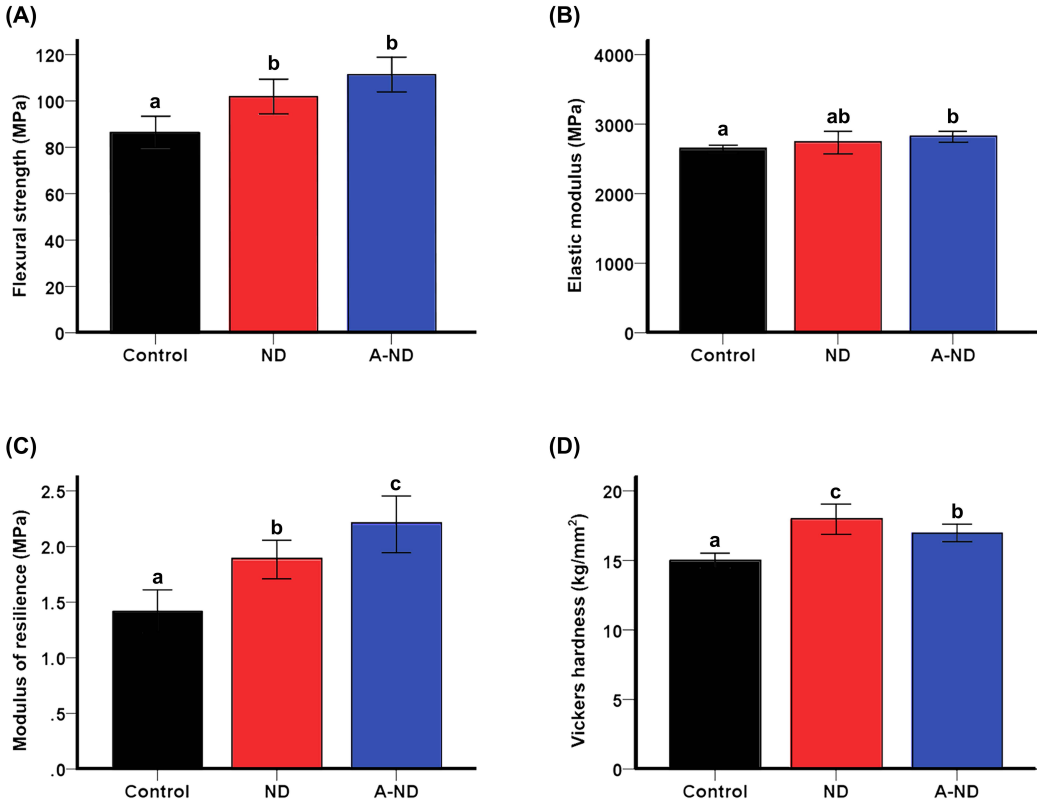

Figure 11. Nanocomposite response to hydrothermal fatigue. Comparing the (A) flexural strengths, (B) elastic moduli, (C), moduli of resilience (D) Vickers hardness of the various groups of samples. Different lowercase letters indicate significant differences. Statistical analysis with one-way ANOVA and post-hoc analysis with Tukey's test was conducted to compare the groups. Dissimilar letters indicate significant differences from each group ($p < 0.05$).

연세대학교
YONSEI UNIVERSITY

Table 2. Mean values of strength, modulus, and microhardness of the various groups and their standard deviations (SDs) after thermocycling

Groups	Flexural Strength (MPa)	Elastic modulus (MPa)	Modulus of Resilience (MPa)	Vickers Microhardness (kg/mm^2)
Control	86.35 ± 6.78^{a}	2640.00 ± 50.25^{a}	1.41 ± 0.19^{a}	14.98 ± 0.52^{a}
ND	101.76 ± 7.44^{b}	2735.08 ± 158.70^{ab}	1.88 ± 0.17^{b}	17.96 ± 1.07^{c}
A-ND	111.21 ± 7.43^{b}	2816.25 ± 73.83^{b}	2.20 ± 0.25^{c}	16.98 ± 0.62^{b}

Statistical analysis with one-way ANOVA and post-hoc analysis with Tukey's test was conducted to compare the groups. In the vertical column, dissimilar letters indicate significant differences from each group ($p < 0.05$).

6. Bacterial resistance

The confocal imaging of the bacterial biofilm exhibited distinctive features between the control and ND/A-ND groups (Figure 12A). The biofilm thickness (Figure 12B) and biomass (Figure 12C) after 48 h were observed to be highest in the control group and significantly less in ND- and A-ND-incorporated groups, showing statistically significant ($p < 0.01$) differences. There was no significant difference in the thickness and biomass of the biofilms between ND and A-ND.

연세대학교
YONSEI UNIVERSITY

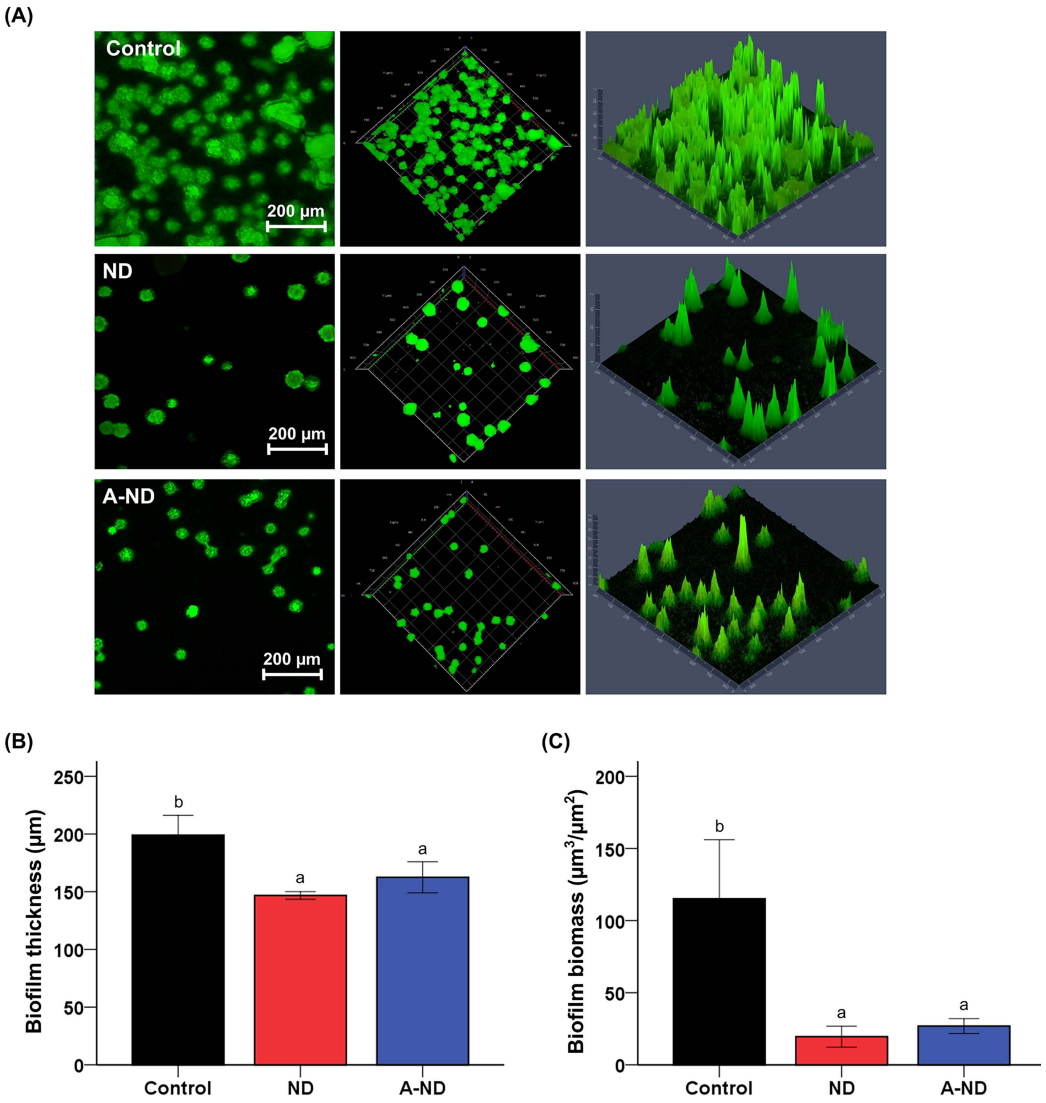

Figure 12. Bacterial biofilm resistance of the nanocomposite. Representative live/dead staining images of the biofilms (A) attached on the surfaces of control and ND- and A-ND incorporated nanocomposite. Quantitative analysis of the thickness (B) and biomass (C) of the biofilms. Statistical analysis with one-way ANOVA and post-hoc analysis with Tukey's test was conducted to compare the groups. In the vertical column, dissimilar letters indicate significant differences from each group ($p < 0.05$).

연세대학교
YONSEI UNIVERSITY

7. Additive manufacturing trueness

A morphometric comparison of the three groups verified the absence of any significant morphological changes in printing accuracy due to nanofiller incorporation. The observed mean RMS values for the control (46.9 ± 2 μm), ND-incorporated (47.5 ± 2.7 μm), and A-ND-incorporated (46.0 ± 3.2 μm) groups were not significantly different (p = 0.732) when compared statistically. The results were visually appraised by superimposing the scanned images with the reference CAD file to produce color maps showing deviations in the ±200 μm range (Figure 13).

연세대학교
YONSEI UNIVERSITY

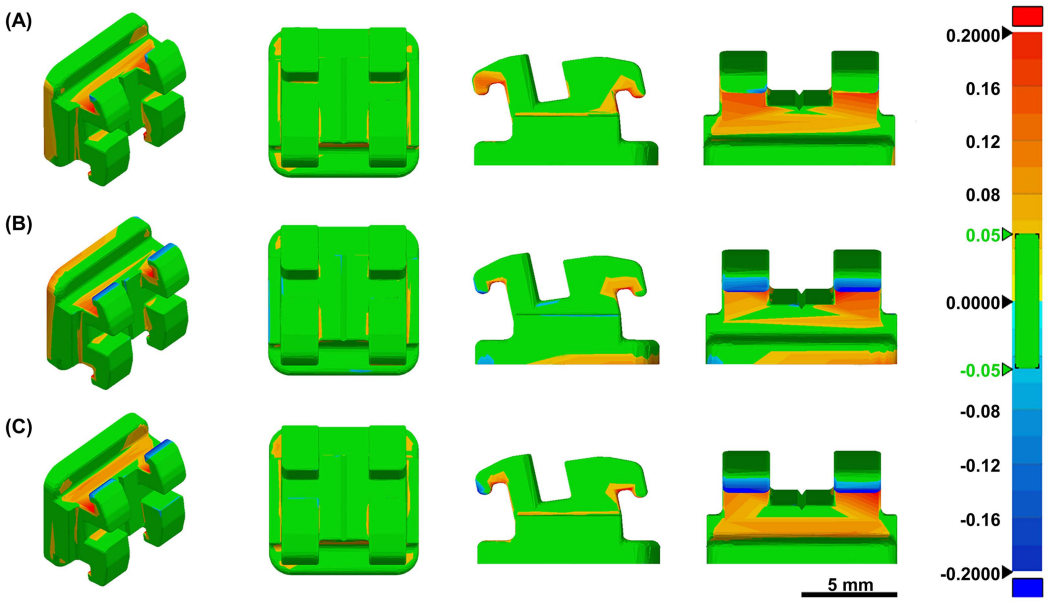

Figure 13. Trueness analysis of orthodontic bracket geometry. Superimposed optically scanned surfaces of 3D-printed bracket designs and the reference CAD model. (A) Control, (B) ND-incorporated, and (C) A-ND-incorporated. Scale bar: 5 mm. Color gradient scale bar: -200 μm (blue) to +200 μm (red).

연세대학교
YONSEI UNIVERSITY

IV. DISCUSSION

In fabrication of resin-based nanocomposites, achieving a homogenous dispersion of carbon nanoparticles, such as the ND, is challenging, and methods such as high-power sonication and shear mixing have been suggested (Pentecost et al., 2010). However, the choice of method has been based on the suitability of the polymer material used. The surface properties of NDs enable them to be chemically modified and, consequently, form strong covalent bonds in the polymer matrix (Jabeen et al., 2015). However, in the context of polymeric fillers, NDs have been observed to agglomerate leading to poor dispersion and inadequate polymer/ND interactions consequently (Karami et al., 2019). Therefore, to best use the features of NDs as fillers for polymers such as PMMA, it is imperative that the nanoparticles are highly uniformly dispersed. However, due to surface chemistry of ND, deagglomeration beyond the microscale with simple mechanical methods alone is challenging; hence, surface modification is required (Pedroso-Santana et al., 2017). Surface functionalization of the ND can aid deagglomeration process and improve stability in organic media by reducing the surface energy and inter-particle bonding of nanoparticles (Lai and Barnard, 2011; Liu et al., 2015).

In a previous study, direct vigorous stirring and sonication of the resin was reported to mix microdiamond particles (Kalsoom et al., 2016). However, according to the observations of Suave *et al*. direct resin sonication can lead to a reduction in oligomer

연세대학교
YONSEI UNIVERSITY

concentration due to the lysing of chains (Suave et al., 2009). Hence, in the present study, one of the most used solvents, chloroform was used to disperse NDs with high power sonication prior to mechanical mixing and degassing based on earlier optimization protocols (Garg et al., 2010; Prolongo et al., 2008; Suave et al., 2009). The other key factors that need to be considered to avoid agglomeration and uneven dispersion are surface homogenization and the concentration of the incorporated NDs. The properties of PMMA (Protopapa et al., 2011), epoxy (Ayatollahi et al., 2012; Rakha et al., 2014), and poly(vinyl alcohol) (Yamamoto et al., 2019) were reportedly improved with less than 0.2 wt.% ND incorporation. Moreover, in an earlier study with auto polymerizing PMMA 0.1 wt.% ND had shown significant improvement in mechanical properties (Mangal et al., 2019). Therefore, in the present study, both the ND- and A-ND-incorporated nanocomposites were fabricated with a 0.1 wt.% ND concentration.

Intraoral appliances in orthodontics are prescribed for long continuous periods of wear; consequently, improvements in surface wettability will lead to improvements in retention between oral mucosa and the intaglio surface (Choi et al., 2020). In the present study, the surface features of the ND were observed to influence the features of the polymer surface, with markedly significant reductions in water contact angle observed for both the ND- and A-ND-nanocomposite groups, in agreement with the observations of a previous study and highlighting the influence of the hydrophilic nature of diamond (Waheed et al., 2019). The difference between the ND- and A-ND-incorporated groups, however, can be attributed to changes in the surface chemistry resulting from the addition

연세대학교
YONSEI UNIVERSITY

of amino groups, which reduces the surface reactivity of the oxygenated outer shell compared to that of pure ND, as previously described (Lechleitner et al., 2008).

In addition, it is plausible that the surface chemistry influences the water solubility of the polymer, with low or negative values observed for the nanocomposite groups. Sorption and solubility in water are critical properties with respect to long-term bonded appliances, such as orthodontic brackets and tubes. High water sorption can lead to plasticization of the polymer and a reduction in the internal-stress threshold, leading to premature failure. In this study, however, reductions in both sorption and water solubility were observed. Despite negative water-solubility values for the nanocomposite groups, the absence of elution, it does not reflect and can be reasonably be ascribed to the formation of bonds to the polar groups of polymer chains, the expression of very low solubility, or early rapid desorption (Lopes et al., 2009; Tuna et al., 2008).

NDs mimic the properties of bulk diamond, and these properties were observed in the nanocomposite polymers. Resin-based biomedical appliances are used in intraoral environments, as bonded attachments, and removable appliances. Properties that enable these appliances to withstand a variety of mechanical insults, such as abrasion and compression, during their use are essential. Tribo-mechanical testing provides an objective way of comparing force limits and describing the elastic nature of these materials. In agreement with the findings of previous studies (Ayatollahi et al., 2012; Kalsoom et al., 2016; Neitzel et al., 2011), the addition of NDs was observed to increase mechanical strength by *ca.* 31% and the elastic modulus by *ca.*12%. Among the two

연세대학교
YONSEI UNIVERSITY

nanocomposite groups, the A-ND-incorporated group exhibited higher values, which is ascribable to stronger covalent linkages and the somewhat better mono-dispersed state of the A-NDs in the polymer, as evidenced by TEM (Jee and Lee, 2009).

The findings were also validated through the notable improvements in the moduli of resilience of the nanocomposites, which indicate an augmented capacity to absorb energy prior to deformation, as observed by SEM, where increased coarseness (A-ND >ND) was observed in the fracture surfaces. The rough surface corresponds to the energy dissipation pattern of the propagating crack, which bows around the inorganic filler particles to create step defects (Galehdari and Kelkar, 2017; McGrath et al., 2008).

Furthermore, in the surface hardness results a similar trend of significantly higher hardness observed for the nanocomposite test groups. However, in contrast to a previous study (Jee and Lee, 2011), the ND-incorporated group showed a slightly higher surface hardness compared to the A-ND group, although statistically comparable.

In a dynamic oral environment, the acrylate based PMMA dental appliances experience conditions that expose the surface to repeated wear. At the same time, polymer-based active appliances (*e.g.*, orthodontic attachments like brackets and tubes) experience friction and wear by interacting with metal wires such as stainless steel or titanium during treatment, often reducing the longevity of the appliance (Eliades and Bourauel, 2005).

연세대학교
YONSEI UNIVERSITY

Nanosized fillers exhibit significant reinforcement effects on the composites. With the reduction in particle size, a subsequent increase in the surface area facilitates better bonding between the particles and matrix (Lim et al., 2009). The round-shaped nanosized diamond particles with the surface properties of chemical stability and superior hardness have been considered as one of the ideal fillers in the development of the nanocomposites (Karami et al., 2019). In modifying the ND-based polymers, improvements in the tribological properties of the composites were observed in terms of the coating, as a lubricant, and even as a bulk material (Zhai et al., 2017). Similar results were observed when NDs were incorporated into the PMMA-based dental polymers, demonstrating a significant improvement in the bulk properties (Al-Harbi et al., 2019; Jee and Lee, 2011).

In a dynamic oral environment, the acrylate based PMMA dental appliances experience conditions that expose the surface to repeated wear. At the same time, polymer-based active appliances (*e.g.*, orthodontic attachments (bracket or tubes) and occlusal splints) experience friction and wear by interacting with metallic counter surfaces during therapeutic use, often responsible for reducing the longevity of the appliance (Eliades and Bourauel, 2005). In progressively analyzing the efficacy of 3D-printed dental appliances, the evaluation of the surface tribological behavior is critical owing to the aforementioned reasons. Hence, in the present study, the evaluation of frictional and wear behavior was conducted.

연세대학교
YONSEI UNIVERSITY

Since topographical features can influence the COF analysis, the surface roughness of the different groups was evaluated to rule-out presence of any significant differences. The subsequent testing showed a tremendous reduction in the COF when a small quantity of ND was added. The reduction in COF largely correlated with that observed by Ayatollahi et al., exhibiting a significant improvement in the wear rate and COF with a low percentage of ND fillers in the epoxy resin (Ayatollahi et al., 2012). Thereafter, any additional increase in the percentage of ND fillers only induced a mild improvement in the wear rate. However, in contrast to the findings obtained by Neitzel et al. (Neitzel et al., 2012a) on the friction and wear behavior with functionalized ND, no significant differences were observed when A-ND was used in this study. The tribological properties of carbon-based nanomaterials depend on the dispersion uniformity in the resin matrix (Myshkin et al., 2005). Resulting from the nanoscale structure of the particles and the associated Van der Waals forces, the ND nanoparticles show an increased tendency towards agglomeration and self-assembly, which hinders dispersion into the polymer matrix (Karami et al., 2019; Neitzel et al., 2012b). Thus, with higher ND content, like that in the study by Neitzel et al. (Neitzel et al., 2012a), the functionalization of the ND can play a significant role in achieving a homogenous dispersion (Jee and Lee, 2009).

Wear is the progressive loss of material due to relative motion between a surface and the contacting substance(s) influenced by parameters such as surface roughness as well as the mechanical, physical, and chemical properties of the interacting bodies (polymers, metal, or composite) (Sulong and Aziz, 1990). The wear of dental appliances

연세대학교
YONSEI UNIVERSITY

has been primarily characterized as adhesive and erosive wear, which influence the longevity and cost of treatment (Turssi et al., 2003). In the oral cavity, the wear of resin-based appliances like orthodontic attachments occurs due to constant multiaxial loading (Park et al., 2018). In this study, the ND- and A-ND-incorporated nanocomposites demonstrated significantly improved wear resistance. Moreover, under a reciprocating load, both the wear rate and wear area exhibited a considerable reduction when compared to the control. This improvement in the wear performance in the polymer matrix containing NDs has been credited to the reduction in the plowing and adhesion of the composite surface to the abrasive counterparts (Ayatollahi et al., 2012).

Furthermore, the notable reduction in the wear and COF could be attributed to the hardness of the nanocomposites following the reinforcement with ND, which is a filler with inherently superior hardness (Neitzel et al., 2012b). An increase in the hardness improves the resistance of the penetration of counter abrasive surfaces, thus retarding the material loss. In addition, the amelioration of the surface wear for polymers has also been linked to the scale and morphology of the particles. The abrasiveness of the nanoparticles was reduced due to the reduction in angularity (Friedrich, 2018), and the particles that were released during abrasion acted as nanopolishing agents that smoothed the surface. This is also believed to contribute to the lowering of the COF (Chang et al., 2008). Though the amount of material removed in the nanocomposites was observed to be much less than control, the presence of wear debris is a known factor that can affect the formation of the transfer layer and rate of wear (de Oliveira et al., 2018). In the present study, the test was

연세대학교
YONSEI UNIVERSITY

conducted under PBS lubrication; however, as no specific methods of debris removal such as micro-pores, brushing, or blowing air were factored, the observations might differ with evaluation in these conditions. It is essential, however, to state that the anisotropic nature of the 3D printed dental materials has a preponderant effect on mechanical performance such as wear (Vayrynen et al., 2016). This denotes a limitation of the current study, which should be considered in future work where further evaluations to accounting for functional multiaxial loading will add to the value.

To simulate the response of the resin-based appliances in the environment of intended use, changes with hydrothermal fatigue were also studied. Simulation replicating the intraoral physical conditions which lead to influence the polymer-based appliance were assessed. In the review by Gale and Darvell, it has been suggested that a mean temperature intraorally ranges from 6 ℃ to 55 ℃ with as much as 10000 cycles of change indicating a year of length (Gale and Darvell, 1999). With such conditions hydrolytic aging occurs which is believed to cause plasticization and lower the mechanical properties of the polymer by causing damage to ester bonds (Pieniak et al., 2019). The observations of the present study were in accordance with the proposed concept and reduction in mechanical properties was noted. However, nanocomposites specimens were superior to the control group and A-ND showed significantly higher modulus of resilience after the hydrothermal insult.

Furthermore, with the ultimate aim of fabricating individualized appliances, the quality of fit is an essential aspect in 3D-printed intraoral appliances. This is of added

연세대학교
YONSEI UNIVERSITY

significance when considering the complex design requirements such as for an orthodontic bracket. Therefore, in the present study, a quality quantification test was used to analyze printed outcomes. A 3D printed bracket design to verify that modification of the resin polymer composition does not change the output quality. A low RMS deviation value corresponds to superior trueness, as demonstrated in earlier studies using similar methodologies that compare offset errors (Jeong et al., 2018; Kim et al., 2018). The absence of any significant differences in trueness suggests that similar printing conditions to those currently used for commercial resin provides reproducible outcomes. However, the test only compared three groups, and the printer and associated design factors also concomitantly influence the output.

During long-term intra-oral use, PMMA-based appliances also undergo interaction with the oral microbiome. *S. mutans* has a strong affinity to hydroxyapatite and forms one of the early colonizers that increases the risk for tooth decay. Orthodontic brackets when retained for a prolonged period and provide sites for the attachment and growth of the *S. mutans* colonies, following protein binding by hydrophobic interactions (Ahn et al., 2003). The attached colonies led to the formation of a biofilm, which underwent calcification under acidic micro-environments, thus resulting in the intra-oral aging of orthodontic appliances (Eliades and Bourauel, 2005). The calcified biofilm deters the sliding mechanics due to varying friction.

Additionally, the bacterial interactions with the intra-oral appliances have been linked to their surface energy and topography. Rough surfaces provide preferential

연세대학교
YONSEI UNIVERSITY

retention of bacteria by offering protection against shear forces (Bollenl et al., 1997). Moreover, a change in the roughness above 2 μm has been suggested to dramatically increase bacterial colonization on the resin surface (Quirynen et al., 1992). Thus, both surface physical characteristics and hydrophobicity can critically influence the biofilm formation on biomaterials (De-la-Pinta et al., 2019). Given the hydrophilic and antibacterial nature of the ND-incorporated composites reported in previous literature (Shirani et al., 2019), the ND-incorporated resin matrix could resist the *S. mutans* biofilm formation, as seen in the characterization of our biofilm after 48 h. Although, detailed characterization of changes in surface energy, in correlation to topography as an influence of nanodiamond functionalization form a prospect for further research. Hence, in this study, a synergism of surface hydrophilicity and surface wear resistance was imparted to the PMMA containing the ND, which can potentially enhance the durability of the dental appliances.

Therefore, this study provides a promising solution to overcome the challenge of the intra-oral aging of 3D-printed appliances due to microbial insult. However, since this study was conducted in vitro, the findings must be verified in a potent in vivo environment which factors in three-body wear and role of salivary constituents.

연세대학교
YONSEI UNIVERSITY

V. CONCLUSION

We evaluated the properties of biological grade PMMA for 3D printing with addition of 0.1wt. % of non-functionalized and aminated nanodiamond. The null-hypothesis was rejected based on the statistically significant differences in tribo-mechanical properties observed for the nanodiamond containing groups against the control.

Within the limitation of the study, following conclusion could be drawn (Figure 14):

1. A-ND having better dispersion and improved homogeneity presented a significantly higher physical and mechanical properties specifically, the flexural strength, impact strength, elastic modulus, and modulus of resilience.
2. A-ND also presented with better resistance to hydrothermal fatigue compared to both ND and Control.
3. With addition of both ND and A-ND the tribological properties of coefficient of friction, wear rate and wear loss showed significant reduction against stainless steel and titanium two-body wear conditions.
4. Both nanodiamond fillers presented with significant resistance to *S. mutans* biofilm formation.
5. The addition of nanodiamonds using solvent based mixing, in low weight percentage did not alter the trueness of a complex 3D printed geometry.

연세대학교
YONSEI UNIVERSITY

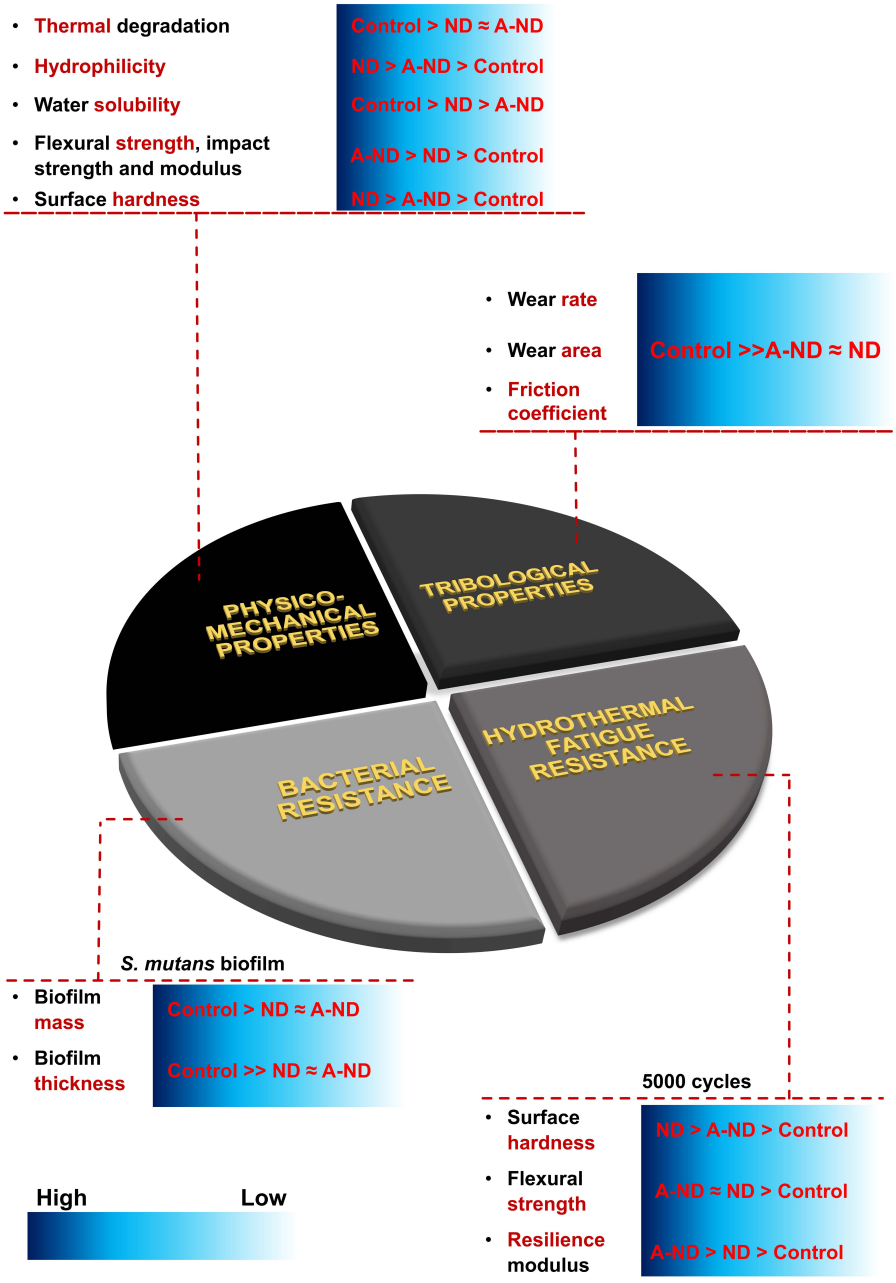

Figure 14. Summarization of the research methodology and outcome. 3D printed PMMA polymer with and without nanodiamond fillers were compared for changes in different physical, mechanical, tribological test and resistance to bacterial biofilm.

연세대학교
YONSEI UNIVERSITY

Therefore, it is possible to conclude that the tribo-mechanical and bacterial resistance of the 3D printing PMMA improve by incorporation of 0.1wt % of nanodiamond and are additionally benefited by amine functionalization of the nanodiamond surface. Despite the limitations of this study, the observation of significant improvement in tribo-mechanical and bacterial resistance of the nanodiamond incorporated PMMA could be helpful in improving the design and quality features of intra-oral appliances including but not limited to splints and retainers.

연세대학교
YONSEI UNIVERSITY

VI. REFERENCES

Aghajani Derazkola H, Simchi A (2018). Effects of alumina nanoparticles on the microstructure, strength and wear resistance of poly(methyl methacrylate)-based nanocomposites prepared by friction stir processing. *Journal of the Mechanical Behavior of Biomedical Materials* 79: 246-253.

Ahn SJ, Kho HS, Kim KK, Nahm DS (2003). Adhesion of oral streptococci to experimental bracket pellicles from glandular saliva. *American Journal of Orthodontics and Dentofacial Orthopedics* 124(2): 198-205.

Al-Harbi FA, Abdel-Halim MS, Gad MM, Fouda SM, Baba NZ, AlRumaih HS, et al. (2019). Effect of nanodiamond addition on flexural strength, impact strength, and surface roughness of PMMA denture base. *Journal of Prosthodontics* 28(1): e417-e425.

Al Mortadi N, Jones Q, Eggbeer D, Lewis J, Williams RJ (2015). Fabrication of a resin appliance with alloy components using digital technology without an analog impression. *Am J Orthod Dentofacial Orthop* 148(5): 862-867.

Amides I, Co ÀÀ, Miller FA (2003). Amides, Carboxylate Ion, and C—O single bonds. *Course Notes on the Interpretation of Infrared and Raman Spectra*: 205-215.

Atzeni E, Salmi A (2012). Economics of additive manufacturing for end-usable metal parts. *International Journal of Advanced Manufacturing Technology* 62(9-12): 1147-1155.

Ayatollahi MR, Alishahi E, Doagou-R S, Shadlou S (2012). Tribological and mechanical properties of low content nanodiamond/epoxy nanocomposites. *Composites Part B: Engineering* 43(8): 3425-3430.

Balazs AC, Emrick T, Russell TP (2006). Nanoparticle polymer composites: Where two small worlds meet. *Science* 314(5802): 1107-1110.

연세대학교
YONSEI UNIVERSITY

Bollenl CML, Lambrechts P, Quirynen M (1997). Comparison of surface roughness of oral hard materials to the threshold surface roughness for bacterial plaque retention: A review of the literature. *Dental Materials* 13(4): 258-269.

Carter SD, Costa PF, Vaquette C, Ivanovski S, Hutmacher DW, Malda J (2017). Additive biomanufacturing: an advanced approach for periodontal tissue regeneration. *Annals of biomedical engineering* 45(1): 12-22.

Chang L, Zhang Z, Ye L, Friedrich K (2008). CHAPTER 3 - Synergistic effects of nanoparticles and traditional tribo-fillers on sliding wear of polymeric hybrid composites. In: Tribology and Interface Engineering Series. Friedrich K, Schlarb AK, eds. Elsevier. p. 35-61.

Cheng Y, Feng G, Moraru CI (2019). Micro- and nanotopography sensitive bacterial attachment mechanisms: A review. *Frontiers in Microbiology* 10: 191.

Choi W, Jin J, Park S, Kim JY, Lee MJ, Sun H, et al. (2020). Quantitative interpretation of hydration dynamics enabled the fabrication of a zwitterionic antifouling surface. *ACS Appl Mater Interfaces* 12(7): 7951-7965.

De-la-Pinta I, Cobos M, Ibarretxe J, Montoya E, Eraso E, Guraya T, et al. (2019). Effect of biomaterials hydrophobicity and roughness on biofilm development. *Journal of Materials Science: Materials in Medicine* 30(7): 77.

de Oliveira MM, Hammes G, Binder C, Klein AN, de Mello JDB (2018). Solid lubrication in fluid film lubrication. *Lubrication Science* 30(3): 102-115.

El Bahra S, Ludwig K, Samran A, Freitag-Wolf S, Kern M (2013). Linear and volumetric dimensional changes of injection-molded PMMA denture base resins. *Dental Materials* 29(11): 1091-1097.

Eliades T, Bourauel C (2005). Intraoral aging of orthodontic materials: The picture we miss and its clinical relevance. *American Journal of Orthodontics and Dentofacial Orthopedics* 127(4): 403-412.

연세대학교
YONSEI UNIVERSITY

Epstein AK, Wong TS, Belisle RA, Boggs EM, Aizenberg J (2012). Liquid-infused structured surfaces with exceptional anti-biofouling performance. *Proceedings of the National Academy of Sciences. USA* 109(33): 13182-13187.

Feng ZY, Li Y, Hao L, Yang YH, Tang T, Tang DN, et al. (2019). Graphene-reinforced biodegradable resin composites for stereolithographic 3D printing of bone structure scaffolds. *Journal of Nanomaterials, 2019*.

Fernandes N, van den Heever J, Hoogendijk C, Botha S, Booysen G, Els J (2016). Reconstruction of an extensive midfacial defect using additive manufacturing techniques. *Journal of Prosthodontics-Implant Esthetic and Reconstructive Dentistry* 25(7): 589-594.

Friedrich K (2018). Polymer composites for tribological applications. *Advanced Industrial and Engineering Polymer Research* 1(1): 3-39.

Gale MS, Darvell BW (1999). Thermal cycling procedures for laboratory testing of dental restorations. *Journal of dentistry.* 27(2): 89-99.

Galehdari NA, Kelkar AD (2017). Effect of neutron radiation on the mechanical and thermophysical properties of nanoengineered polymer composites. *Journal of Materials Research* 32(2): 426-434.

Garg P, Singh BP, Kumar G, Gupta T, Pandey I, Seth RK, et al. (2010). Effect of dispersion conditions on the mechanical properties of multi-walled carbon nanotubes based epoxy resin composites. *Journal of Polymer Research* 18(6): 1397-1407.

Heydorn A, Nielsen AT, Hentzer M, Sternberg C, Givskov M, Ersboll BK, et al. (2000). Quantification of biofilm structures by the novel computer program COMSTAT. *Microbiology,* 146(10), 2395-2407.

연세대학교
YONSEI UNIVERSITY

Ilie N, Hilton TJ, Heintze SD, Hickel R, Watts DC, Silikas N, et al. (2017). Academy of dental materials guidance—Resin composites: Part I—Mechanical properties. *Dental Materials* 33(8): 880-894.

Jabeen S, Kausar A, Muhammad B, Gul S, Farooq M (2015). A review on polymeric nanocomposites of nanodiamond, carbon nanotube, and nanobifiller: structure, preparation and properties. *Polymer-Plastics Technology and Engineering* 54(13): 1379-1409.

Jee AY, Lee M (2009). Surface functionalization and physicochemical characterization of diamond nanoparticles. *Current Applied Physics* 9(2): E144-E147.

Jee AY, Lee M (2011). Mechanical properties of polycarbonate and poly(methyl methacrylate) films reinforced with surface-functionalized nanodiamonds. *Journal of Nanoscience and Nanotechnology* 11(1): 533-536.

Jeong YG, Lee WS, Lee KB (2018). Accuracy evaluation of dental models manufactured by CAD/CAM milling method and 3D printing method. *The Journal of Advanced Prosthodontics* 10(3): 245-251.

Kalsoom U, Peristyy A, Nesterenko PN, Paull B (2016). A 3D printable diamond polymer composite: a novel material for fabrication of low cost thermally conducting devices. *RSC Advances* 6(44): 38140-38147.

Karami P, Salkhi Khasraghi S, Hashemi M, Rabiei S, Shojaei A (2019). Polymer/nanodiamond composites - a comprehensive review from synthesis and fabrication to properties and applications. *Advances in colloid and interface science* 269: 122-151.

Kim SY, Shin YS, Jung HD, Hwang CJ, Baik HS, Cha JY (2018). Precision and trueness of dental models manufactured with different 3-dimensional printing techniques. *American Journal of Orthodontics and Dentofacial Orthopedics* 153(1): 144-153.

연세대학교
YONSEI UNIVERSITY

Kwon JS, Lee MJ, Kim JY, Kim D, Ryu JH, Jang S, et al. (2019). Novel anti-biofouling light-curable fluoride varnish containing 2-methacryloyloxyethyl phosphorylcholine to prevent enamel demineralization. *Scientific Reports* 9(1): 1432.

Lai L, Barnard AS (2011). Stability of nanodiamond surfaces exposed to N, NH, and NH_2. *Journal of Physical Chemistry C* 115(14): 6218-6228.

Lechleitner T, Klauser F, Seppi T, Lechner J, Jennings P, Perco P, et al. (2008). The surface properties of nanocrystalline diamond and nanoparticulate diamond powder and their suitability as cell growth support surfaces. *Biomaterials* 29(32): 4275-4284.

Lee MJ, Kwon JS, Kim JY, Ryu JH, Seo JY, Jang S, et al. (2019). Bioactive resin-based composite with surface pre-reacted glass-ionomer filler and zwitterionic material to prevent the formation of multi-species biofilm. *Dental Materials* 35(9): 1331-1341.

Lim DP, Lee JY, Lim DS, Ann SG, Lyo IW (2009). Effect of reinforcement particle size on the tribological properties of nano-diamond filled polytetrafluoroethylene based coating. *Journal of Nanoscience and Nanotechnology* 9(7): 4197-4201.

Liu MY, Xu DZ, Wang K, Deng FJ, Wan Q, Zeng GJ, et al. (2015). Nanodiamond based supermolecular nanocomposites: preparation and biocompatibility evaluation. *Rsc Advances* 5(117): 96983-96989.

Lopes LG, Jardim Filho Ada V, de Souza JB, Rabelo D, Franco EB, de Freitas GC (2009). Influence of pulse-delay curing on sorption and solubility of a composite resin. *Journal of Applied Oral Science* 17(1): 27-31.

Mangal U, Kim JY, Seo JY, Kwon JS, Choi SH (2019). Novel Poly(Methyl Methacrylate) containing nanodiamond to improve the mechanical properties and fungal resistance. *Materials (Basel)* 12(20): 3438-3438.

연세대학교
YONSEI UNIVERSITY

McGrath LM, Parnas RS, King SH, Schroeder JL, Fischer DA, Lenhart JL (2008). Investigation of the thermal, mechanical, and fracture properties of alumina-epoxy composites. *Polymer* 49(4): 999-1014.

Mochalin VN, Neitzel I, Etzold BJ, Peterson A, Palmese G, Gogotsi Y (2011). Covalent incorporation of aminated nanodiamond into an epoxy polymer network. *ACS Nano* 5(9): 7494-7502.

Mochalin VN, Shenderova O, Ho D, Gogotsi Y (2012). The properties and applications of nanodiamonds. *Nature Nanotechnology* 7(1): 11-23.

Myshkin NK, Petrokovets MI, Kovalev AV (2005). Tribology of polymers: Adhesion, friction, wear, and mass-transfer. *Tribology International* 38(11-12): 910-921.

Neitzel I, Mochalin V, Bares JA, Carpick RW, Erdemir A, Gogotsi Y (2012a). Tribological Properties of Nanodiamond-Epoxy Composites. *Tribology Letters* 47(2): 195-202.

Neitzel I, Mochalin V, Knoke I, Palmese GR, Gogotsi Y (2011). Mechanical properties of epoxy composites with high contents of nanodiamond. *Composite Science and Technology* 71(5): 710-716.

Neitzel I, Mochalin VN, Niu J, Cuadra J, Kontsos A, Palmese GR, et al. (2012b). Maximizing Young's modulus of aminated nanodiamond-epoxy composites measured in compression. *Polymer* 53(25): 5965-5971.

Park JM, Ahn JS, Cha HS, Lee JH (2018). Wear resistance of 3D printing resin material opposing zirconia and metal antagonists. *Materials* 11.

Pedroso-Santana S, Sarabia-Sainz A, Fleitas-Salazar N, Santacruz-Gomez K, Acosta-Elias M, Pedroza-Montero M, et al. (2017). Deagglomeration and characterization of detonation nanodiamonds for biomedical applications. *Journal of Applied Biomedicine* 15(1): 15-21.

연세대학교
YONSEI UNIVERSITY

Pentecost A, Gour S, Mochalin V, Knoke I, Gogotsi Y (2010). Deaggregation of nanodiamond powders using salt- and sugar-assisted milling. *ACS applied materials & interfaces,* 2(11): 3289-3294.

Pieniak D, Przystupa K, Walczak A, Niewczas AM, Krzyzak A, Bartnik G, et al. (2019). Hydro-thermal fatigue of polymer matrix composite biomaterials. *Materials (Basel)* 12(22): 3650-3650.

Prolongo SG, Burón M, Gude MR, Chaos-Morán R, Campo M, Ureña A (2008). Effects of dispersion techniques of carbon nanofibers on the thermo-physical properties of epoxy nanocomposites. *Composites Science and Technology,* 68(13): 2722-2730.

Protopapa P, Kontonasaki E, Bikiaris D, Paraskevopoulos KM, Koidis P (2011). Reinforcement of a PMMA resin for fixed interim prostheses with nanodiamonds. *Dental Materials Journal* 30(2): 222-231.

Quirynen M, Marechal M, Busscher HJ, Weerkamp AH, Darius PL, Steenberghe D (1992). The influence of surface free energy and surface roughness on early plaque formation. *Journal of Clinical Periodontology* 17(3): 138-144.

Rakha SA, Ali N, Haleem YA, Alam F, Khurram AA, Munir A (2014). Comparison of mechanical properties of acid and uv ozone treated nanodiamond epoxy nanocomposites. *Journal of Materials Science & Technology* 30(8): 753-758.

Shirani A, Hu Q, Su Y, Joy T, Zhu D, Berman D (2019). Combined tribological and bactericidal effect of nanodiamonds as a potential lubricant for artificial joints. *ACS Applied Materials & Interfaces* 11: 43500-43508.

Suave J, Coelho LAF, Amico SC, Pezzin SH (2009). Effect of sonication on thermo-mechanical properties of epoxy nanocomposites with carboxylated-SWNT. *Materials Science and Engineering: A* 509(1-2): 57-62.

연세대학교
YONSEI UNIVERSITY

Sulong MZAM, Aziz RA (1990). Wear of materials used in dentistry: A review of the literature. *Journal of Prosthetic Dentistry* 63(3): 342-349.

Thaweboon S, Thaweboon B (2019). In vitro study of streptococcus mutans biofilm formation on vanillin-incorporated orthodontic PMMA resin. *Key Engineering Materials*, 801, pp. 9-14). Trans Tech Publications Ltd

Tuna SH, Keyf F, Gumus HO, Uzun C (2008). The evaluation of water sorption/solubility on various acrylic resins. *European Journal of Dentistry* 2(3): 191-197.

Turssi CP, De Moraes Purquerio B, Serra MC (2003). Wear of dental resin composites: insights into underlying processes and assessment methods - A review. *Journal of Biomedical Materials Research - Part B Applied Biomaterials* 65: 280-285.

van Noort R (2012). The future of dental devices is digital. *Dental Materials* 28(1): 3-12.

Vayrynen VO, Tanner J, Vallittu PK (2016). The anisotropicity of the flexural properties of an occlusal device material processed by stereolithography. *The Journal of Prosthetic Dentistry* 116(5): 811-817.

Waheed S, Cabot JM, Smejkal P, Farajikhah S, Sayyar S, Innis PC, et al. (2019). Three-dimensional printing of abrasive, hard, and thermally conductive synthetic microdiamond-polymer composite using low-cost fused deposition modeling printer. *ACS applied materials & interfaces* 11(4): 4353-4363.

Wang X, Jiang M, Zhou Z, Gou J, Hui D (2017). 3D printing of polymer matrix composites: A review and prospective. *Composites Part B: Engineering* 110: 442-458.

Yamamoto BE, Trimble AZ, Minei B, Nejhad MNG (2019). Development of multifunctional nanocomposites with 3-D printing additive manufacturing and

연세대학교
YONSEI UNIVERSITY

low graphene loading. *Journal of Thermoplastic Composite Materials* 32(3): 383-408.

Yu P, Xu Z, Arola DD, Min J, Zhao P, Gao S (2017). Effect of acidic agents on the wear behavior of a polymer infiltrated ceramic network (PICN) material. *Journal of the Mechanical Behavior of Biomedical Materials* 74: 154-163.

Zhai W, Srikanth N, Kong LB, Zhou K (2017). Carbon nanomaterials in tribology. *Carbon N Y* 119: 150-171.

Zhang QW, Mochalin VN, Neitzel I, Knoke IY, Han JJ, Klug CA, et al. (2011). Fluorescent PLLA-nanodiamond composites for bone tissue engineering. *Biomaterials* 32(1): 87-94.

Zhou ZR, Yu HY, Zheng J, Qian LM, Yan Y (2013). Dental biotribology. *Dental Biotribology*: 1-177.

연세대학교
YONSEI UNIVERSITY

ABSTRACT (Korean)

나노다이아몬드를 혼합한 3D 프린팅 폴리메틸메타크릴레이트로 제작된 구강 내 장치의 내마모성 및 항균성

(지도 교수: 최 성 환)

연세대학교 대학원 치의학과

만갈 웃커시

임상에서 3D 프린팅된 구강 내 장치가 적용되기 위해서는 역동적인 구강 내 환경에서 파손되지 않고 오랜기간 사용될 수 있어야 한다. 본 연구는 우수한 강도, 화학적 안정성 및 생체적합성을 지닌 아민화된 나노-다이아몬드(A-ND)를 아크릴레이트 기반 3D 프린팅 재료와 혼합한 후 그에 따른 물리 · 기계적, 생물학적 특성을 평가하였다.

본 연구에서는 UV 경화형 아크릴레이트 기반 수지를 사용하였고, 이를 클로로포름를 이용하여 분산시킨 고순도 나노다이아몬드(ND) 또는 A-ND 다 0.1 % 질량비로 각각 혼합하여 ND 및 A-ND 함유 나노복합체를 제작하였다. 변형되지 않은 수지는 ND 및 A-ND 혼입 수지와 비교하기 위한 대조군으로 사용되었다.

연세대학교
YONSEI UNIVERSITY

UV 경화형 아크릴레이트 기반 수지와 혼합한 결과 A-ND 나노 입자는 ND 에 비해 입자가 균일하게 분산되었고, 응집현상이 감소하였다. ND 및 A-ND 나노복합체는 대조군에 비해 통계적으로 유의하게 낮은 접촉각($p < 0.001$) 및 용해도($p < 0.05$)를 보였다. A-ND 를 함유한 나노복합체는 ND 를 함유한 나노복합체와 대조군에 비해 굴곡강도($p < 0.001$), 탄성계수($p<0.01$) 및 충격강도($p<0.001$)가 현저하게 증가하였다. 나노복합체 그룹 모두에서 대조군에 비해 표면의 비커스 경도가 통계적으로 유의하게 증가하였다($p < 0.001$). 또한 열순환에 의한 시효처리 (aging) 후 굴곡강도, 탄성계수 및 표면경도 또한 대조군에 비해서 유의하게 개선됨을 확인하였다($p < 0.001$).

티타늄 또는 스테인리스 스틸로 제작된 구(ball)를 사용하여 시편을 마모시킴으로써 마찰과 마모에 의한 저항성 시험을 수행한 결과, 티타늄 구를 사용하였을 때 A-ND 나노복합체의 마찰계수는 대조군과 유사하였지만 ND 보다는 낮았고 ($p < 0.01$), ND 및 A-ND 나노복합체 그룹 모두에서 대조군에 비해 내마모성이 향상되었다($p <0.001$). 또한 ND 및 A-ND 나노복합체 모두에서 대조군에 비해 뮤탄스 연쇄상구균(*Streptococcus mutans*)에 의한 생물막 형성이 유의하게 감소하였다($p <0.01$).

마지막으로 ND 및 A-ND 나노복합체로 제조된 3D 프린팅 교정용 브라켓 가공물의 정확도 분석을 시행하였을 때 대조군과 유의한 차이가 없음을 확인하였다.

연세대학교
YONSEI UNIVERSITY

따라서, UV 로 경화된 폴리메틸메타크릴레이트 수지에 0.1 % 질량비로 A-ND 를 혼합하면 기계적 물성, 내마모성 및 항균성이 크게 향상되어 생체 의료용 3D 프린팅 소재로 사용하는데 적합함을 확인할 수 있었다.

핵심되는 말: 폴리메틸메타크릴레이트; 나노다이아몬드; 나노복합체; 3D 프린팅; 마찰계수; 내마모성; 기계적 특성; 뮤탄스 연쇄상구균